Sensing the electrical properties of roots: A review

S. Ehosioke, F. Nguyen, S. Rao, Thomas Kremer, E. Placencia-Gomez, J.A. Huisman, A. Kemna, M. Javaux, S. Garré

Received: 5 March 2020 | Accepted: 1 October 2020

DOI: 10.1002/vzj2.20082

Vadose Zone Journal

SPECIAL SECTION: AGROGEOPHYSICS: GEOPHYSICS TO INVESTIGATE SOIL–PLANT–ATMOSPHERE INTERACTIONS & SUPPORT AGRICULTURAL MANAGEMENT

Sensing the electrical properties of roots: A review

Solomon Ehosioke[1,2] | **Frédéric Nguyen**[1] | **Sathyanarayan Rao**[3] | **Thomas Kremer**[4] | **Edmundo Placencia-Gomez**[1] | **Johan Alexander Huisman**[5] | **Andreas Kemna**[6] | **Mathieu Javaux**[3,5] | **Sarah Garré**[2,7]

[1] Urban and Environmental Engineering, Liège Univ. (ULiège), Liège, Belgium

[2] Gembloux Agro-Bio Tech, Liège Univ. (ULiège), Gembloux, Belgium

[3] Earth and Life Institute, Environmental Science, Univ. Catholique de Louvain, Louvain-la-Neuve, Belgium

[4] CNRS, LPG, Univ. of Nantes, Univ Angers, UMR 6112, Nantes F-44000, France

[5] Agrosphere (IBG 3), Forschungszentrum Jülich, Jülich, Germany

[6] Geophysics Section, Institute of Geosciences, Univ. of Bonn, Germany

[7] Flemish Research Institute for Agriculture, Fisheries, and Food (ILVO), Melle, Belgium

Correspondence
Solomon Ehosioke, Urban and Environmental Engineering, Liège Univ. (ULiège), Liège, Belgium.
Email: solomon.ehosioke@uliege.be

Funding information
Deutsche Forschungsgemeinschaft, Grant/Award Numbers: EXC 2070, -, 390732324, -, Phenorob; Fonds De La Recherche Scientifique - FNRS, Grant/Award Number: PDR-23638781

Abstract

Thorough knowledge of root system functioning is essential to understand the feedback loops between plants, soil, and climate. In situ characterization of root systems is challenging due to the inaccessibility of roots and the complexity of root zone processes. Electrical methods have been proposed to overcome these difficulties. Electrical conduction and polarization occur in and around roots, but the mechanisms are not yet fully understood. We review the potential and limitations of low-frequency electrical techniques for root zone investigation, discuss the mechanisms behind electrical conduction and polarization in the soil–root continuum, and address knowledge gaps. A range of electrical methods for root investigation is available. Reported methods using current injection in the plant stem to assess the extension of the root system lack robustness. Multi-electrode measurements are increasingly used to quantify root zone processes through soil moisture changes. They often neglect the influence of root biomass on the electrical signal, probably because it is yet to be well understood. Recent research highlights the potential of frequency-dependent impedance measurements. These methods target both surface and volumetric properties by activating and quantifying polarization mechanisms occurring at the root segment and cell scale at specific frequencies. The spectroscopic approach opens up a range of applications. Nevertheless, understanding electrical signatures at the field scale requires significant understanding of small-scale polarization and conduction mechanisms. Improved mechanistic soil–root electrical models, validated with small-scale electrical measurements on root systems, are necessary to make further progress in ramping up the precision and accuracy of multi-electrode tomographic techniques for root zone investigation.

Abbreviations: ARSA, absorbing root surface area; DC, direct current; ECF, extracellular fluids; EDL, electrical double layer; EIM, earth impedance method; EIS, electrical impedance spectroscopy; EIT, electrical impedance tomography; ERM, electrical resistance measurements; ERT, electrical resistivity tomography; ICF, intracellular fluids; MALM, mise-a-la-masse; PCA, principal component analysis; SIP, spectral induced polarization.

1 | INTRODUCTION

The rhizosphere provides the necessary nutrients, water, and anchorage for plants and is one of the most active parts of soil in terms of nutrient and carbon cycling and maintaining biodiversity (De-la-Peña & Loyola-Vargas, 2014; Nguyen, 2009). It is home to numerous interactions between soil, plant, and microorganisms. Understanding rhizosphere processes is therefore crucial for sustainable agriculture and food production. Traditional methods of soil and root investigation such as excavation, soil cores, ingrowth bags, or mini-rhizotrons (Maeght, Rewald, & Pierret, 2013) provide insights into the structure, composition, and variability of the subsurface. However, they have clear limitations in terms of temporal and spatial resolution, mainly caused by the spatial heterogeneity of the root zone and its dynamics. Root growth, plant water and nutrient uptake, and transient boundary water fluxes create highly heterogeneous and dynamic patterns in root and soil properties that can be difficult to capture, even with a high-density network of point sensors (Amundson, Richter, Humphreys, Jobbágy, & Gaillardet, 2007; Jayawickreme, Jobbágy, & Jackson, 2014). In addition, intrusive sampling (e.g., rhizotubes) can interfere with the natural state of the system and may affect the processes being monitored, thereby potentially altering the experimental results.

Geophysical methods offer the possibility to infer properties and structures of the rhizosphere and pedosphere, as well as flow and transport processes at various spatial scales ranging from the single root to the field scale. Geophysical properties can be related to soil state variables (e.g., soil moisture content, salt concentration), soil properties (e.g., clay content, cation exchange capacity), and root properties (e.g., root mass, root surface area) as summarized by Vanderborght et al. (2013). Geophysical methods have been widely used in the past two decades to monitor moisture patterns associated with water flow (Deiana et al., 2007; Huisman, Snepvangers, Bouten, & Heuvelink, 2002; Looms, Jensen, Binley, & Nielsen, 2008; Lu & Sabatier, 2009; Oberdörster, Vanderborght, Kemna, & Vereecken, 2010; Weihermüller, Huisman, Lambot, Herbst, & Vereecken, 2007; Zhou, Shimada, & Sato, 2001) and root water uptake (Beff, Günther, Vandoorne, Couvreur, & Javaux, 2013; Cassiani, Boaga, Vanella, Perri, & Consoli, 2015; Dick, Tetzlaff, Bradford, & Soulsby, 2018; Garré, Javaux, Vanderborght, Pages, & Vereecken, 2011; Jayawickreme, Van Dam, & Hyndman, 2008; Mares, Barnard, Mao, Revil, & Singha, 2016; Michot et al., 2003; Srayeddin & Dousssan, 2009; Vanella et al., 2018). The application of geophysical techniques in an agricultural context to study how agricultural production is affected by environmental variables (e.g., water availability, salinity) and agricultural management (e.g., impact of fertilizer and irrigation application), as well as to study fundamental soil–root interactions, is now referred to as "agrogeophysics" (Allred, Daniels, & Ehsani, 2008; Vereecken, Binley, Cassiani, Revil, & Titov, 2007).

Core Ideas

- Electrical methods offer a noninvasive approach for root investigation.
- Impedance measurements at different frequencies are preferable due to more information content.
- Interpretation of impedance spectra at the microscopic level needs to be considered.

Various agrogeophysical applications have been reported in the literature, ranging from mapping of soil compaction or determination of plow-pan depth (Besson, Cousin, Samouëlian, Boizard, & Richard, 2004; Doolittle, Sudduth, Kitchen, & Indorante, 1994; Kitchen, Sudduth, & Drummond, 1999; Lu, Hickey, & Sabatier, 2004; Jonard et al., 2013) to the assessment of irrigation efficiency (Tresoldi et al., 2019). Soil mapping for precision agriculture and crop modeling has been realized using on-the-go electrical resistivity tomography (ERT; Andrenelli et al., 2013; Rossi et al., 2013), electromagnetic induction (Brogi et al., 2019; Corwin & Lesch, 2003; Jaynes, Novak, Moorman, & Cambardella, 1995; Kachanoski, Wesenbeeck, & Gregorich, 1988; Robert et al., 1995; Sudduth, Drummond, & Kitchen, 2001; von Hebel et al., 2018), and ground-penetrating radar (Freeland, Yoder, & Ammons, 1998; Ristic, Petrovacki, & Vrtunski, 2014; Yoder, Freeland, Ammons, & Leonard, 2001) Salinity mapping for whole farm planning is also feasible with geophysical methods (Williams, Walker, & Anderson, 2006). One of the key challenges in agrogeophysics is the noninvasive investigation of the spatial distribution of the root system (Amato et al., 2009; Konstantinovic, Wöckel, Schulze Lammers, Sachs, & Martinov, 2007) and its impact on soil state variables. Due to the vital role that root biomass and architecture play in plant breeding, drought tolerance, and carbon sequestration, measurements of root extent and distribution are necessary for proper understanding and modeling of plant growth, root water uptake, and the carbon balance of agricultural systems.

The aim of this review is to provide an overview of the applications of electrical geophysical methods to root investigation, to critically analyze recent accomplishments, and to identify remaining knowledge gaps. We limit ourselves to low-frequency electrical methods, from direct current (DC) to a few tens of kilohertz, due to their potential to investigate individual fine crop roots (diameter <1 mm). Recent reviews focused on imaging of root zone processes (Corona-Lopez, Sommer, Rolfe, Podd, & Rieve, 2019; Zhao et al., 2019), whereas others provided a short summary of the

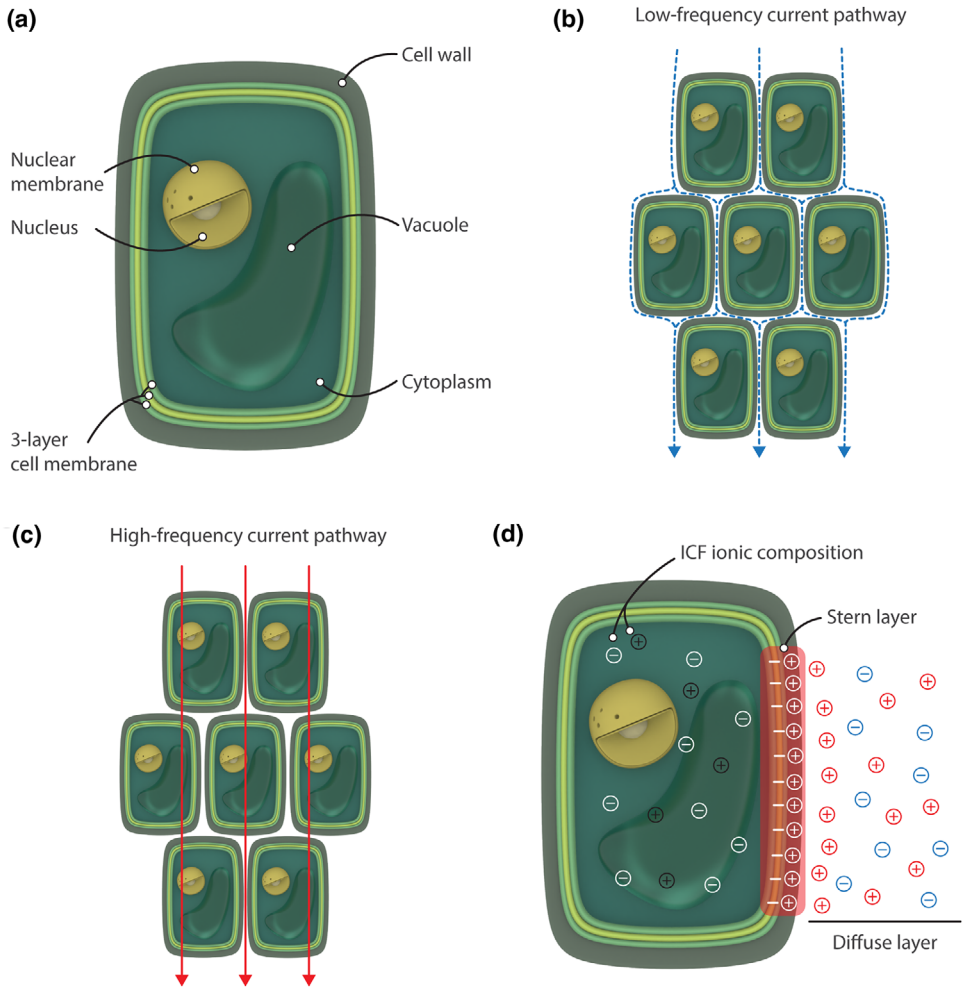

FIGURE 1 Schematic illustration of (a) the plant cell, showing some of the organelles (vacuole, nucleus, and nuclear membranes), the cell wall, and the three-layer (protein-lipid-protein) cell membrane. The frequency-dependent current paths through plant tissues, showing (b) low-frequency current pathway and (c) high-frequency current pathway. (d) Description of counterion polarization mechanism in root segments occurring at low frequencies (Kessouri et al., 2019; Weigand & Kemna, 2019). The strength of the electrical double layer (EDL) polarizability depends on the composition and concentration of ions in the extracellular fluid (ECF) and electric potential distribution at the cell membrane (Kinraide, 2001; Kinraide & Wang, 2010; Wang et al., 2011). ICF, intracellular fluids

application of electrical impedance spectroscopy (EIS) to study various parts of plants (e.g., fruits, vegetables, and leaf water; Jocsac, Vegvari, & Vozary, 2019). To the best of our knowledge, this review is the first attempt to provide a comprehensive overview of all the active electrical methods (based on electric excitation) for root studies that are used by different research communities at various spatial scales. In particular, we reviewed all active electrical methods used to study the capability of roots to conduct electric current and to store electrical energy (in terms of charge separation).

This review is organized as follows. After a brief introduction to electrical conduction and polarization in plants, we will first present the different categories of measurement techniques and highlight their potentials and limitations. After that, we will discuss the common aspects, identify knowledge gaps for this active field of research, and provide suggestions for future research.

1.1 | Electrical conduction and polarization in biological tissue

Biological tissues are made up of cells delimited by membranes. Cells contain tiny cellular structures that perform specific functions (organelles) and intracellular fluids (ICF), together called the cytoplasm (see Figure 1a). In plant cells, membranes are surrounded by cell walls mainly made of polysaccharides. The individual plant cells form a porous network called the apoplast, and the pore space between the cells is filled by extracellular fluids (ECF) (Raven, Johnson, Mason, Losos, & Singer, 2017). The membranes are made of

TABLE 1 Polarization mechanisms in biomaterials

Polarization mechanism	Description	Frequency range
Counterion or ionic polarization	Ionic diffusion in the electrical double layers adjacent to charged surfaces, such as cell membranes, creates polarization (Kao, 2004; Schwan & Takashima, 1991).	α range <20 kHz
Interfacial polarization (Maxwell–Wagner effect)	Restricted movement of ions in the intercellular space as a result of complex structural properties of biological tissue creates high-conductivity zones within the matrix of low conductivity material (e.g., cell interiors surrounded by cell membranes; Kao, 2004; Schwan & Takashima, 1991)	β range (kHz–MHz)
Dipole or orientational polarization	Electrical dipoles can freely orient in response to the application of an electrical field and align themselves with the field (Kao, 2004)	γ range (MHz–GHz)

phospholipids and proteins, which control water and nutrient entry into the cytoplasm due to their selective permeability. This helps to maintain the composition and concentration of the ICF, which is distinctly different from that of the ECF (Raven et al., 2017), as shown in Figure 1d. The radial transport of water and nutrients in roots takes place in the apoplast but also from cell to cell through plasmodesmata (i.e., tiny connections between cells, called the symplastic pathway; Couvreur et al., 2018). These two pathways also play an important role for electrical current flow.

Current conduction within a root depends on the resistance of the apoplast and the extracellular fluid, whereas all membranes and walls play an important role for the storage of electrical charges (polarization). Polarization occurs at the cell membrane interface because charged particles such as Na^+, Ca^{2+}, K^+, and Cl^- ions and amino acids cannot diffuse across the cell membrane. Instead, they can only cross the membranes through ion pumps and ion channels (see the Glossary) whose opening and closing are regulated by the potential difference across the membrane (voltage). Electrical charges at the surface of the cell membrane lead to the formation of an electrical double layer (EDL), consisting of a layer of surface charges of the cell membrane and a layer of associated counterions (Figure 1d) (Kessouri et al., 2019; Kinraide, 2001; Kinraide & Wang, 2010, Weigand & Kemna, 2019). When applying an alternating current, the polarization strength depends on frequency, intensity, and duration of the injection, surface charge density of the cell membrane, transmembrane potential difference, ionic concentration, water content, tissue composition, and tissue health or structural heterogeneity (Ackmann, 1993; Bera, Nagaraju, & Lubineau, 2016; Repo, Cao, Silvennoinen, & Ozier-Lafontaine, 2012). Polarization is expected to occur at both the outer root surface (root–soil interface) and in the inner root system. Here, it is important to realize that the EDL of the outer root surface depends on the concentration of ions in the external fluid, whereas the EDL of the inner root system depends on the ionic composition of the cellular fluid (Weigand & Kemna, 2017, 2019). Polarization is assumed to occur in three frequency ranges, which are referred to as the α, β, and γ range (Prodan, Prodan, & Miller, 2008; Schwan, 1957, 1963, 1988). Table 1 summarizes the three frequency ranges and the specific polarization mechanisms associated to them (Repo et al., 2012; Schwan & Takashima, 1991).

At low frequencies, the voltage gated ion channels of the cell membranes are closed because a low-frequency electric field produces small changes in the membrane potential difference that are too small to significantly alter the properties of the ion channels (Mathie, Kennard, & Veale, 2003). In this case, the EDL prevents any passage of current through the cell membrane (i.e., the impedance of the cell membranes is so high that it does not allow current passage). Instead, the current passes through the apoplast (Bera, Bera, Kar, & Mondal, 2016; Repo et al., 2012), as shown in Figure 1b. In this low-frequency case, the total impedance will be mainly determined by the resistance of the extracellular fluid (Bera, Bera, et al., 2016; Repo et al., 2012); this is termed "counterion polarization" (Table 1). As the frequency increases, the applied electrical field at the outer surface of the membrane changes the transmembrane potential difference that regulates the gating of ion channels and ion fluxes across the cell membranes (Hille, 2001; Kinraide, 2001; Mathie et al., 2003). The opening of ion channels leads to decreased negativity of the membrane surface potential and an increased cation flux into the cell that results in a weaker EDL (Kessouri et al., 2019; Kinraide, 2001; Kinraide & Wang, 2010; Wang, Kinraide, Zhou, Kopittke, & Peijnenburg, 2011; Weigand & Kemna, 2019), and a lower polarizability of the EDL. At these high frequencies, current thus flows through the entire cell and crosses different interfaces (Figure 1c) such that the resulting total impedance will be a combination of the properties of the apoplast and the extracellular fluid, the cell membranes, the cytoplasm, and the ICF (Bera, Bera, et al., 2016; Repo et al., 2012). In this case, the polarization is considered to be interfacial (Table 1). In addition, the influx of cations into the cytoplasm due to concentration gradients that exist across the cell membrane when the ion channels open alters the composition and concentration of the ICF (Kessouri et al., 2019; Weigand & Kemna, 2019), which might explain the large polarization observed in roots at high frequencies (Ehosioke et al., 2018; Kessouri et al., 2019). However, more studies at the root scale,

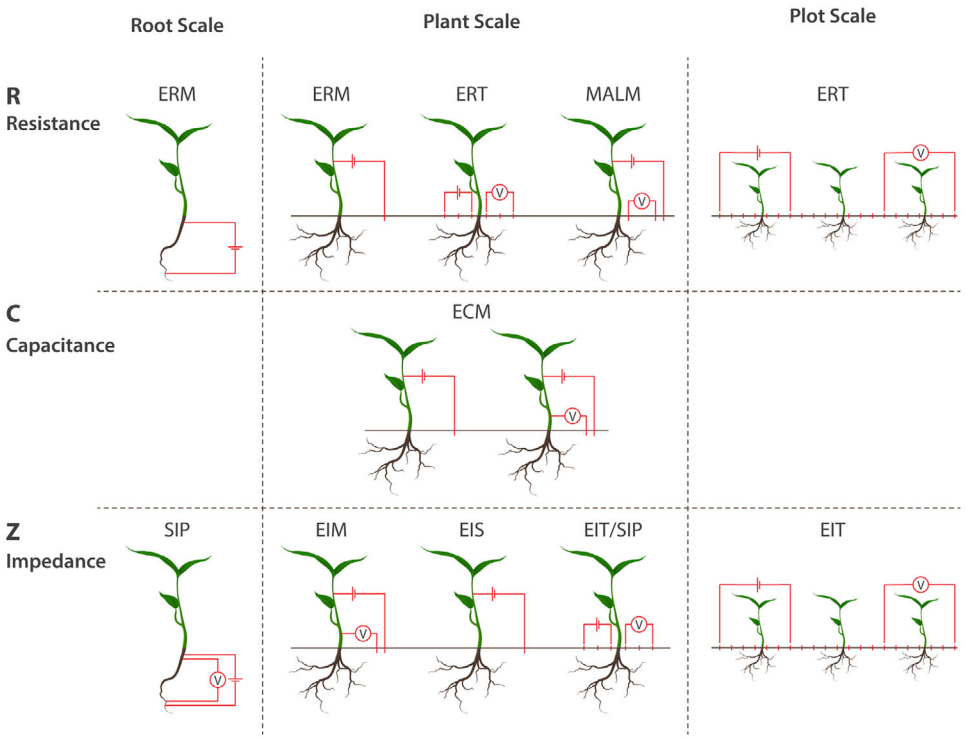

FIGURE 2 Schematic overview of low-frequency electrical methods used for root investigation, classified according to scale and measured parameter: electrical resistance measurement (ERM), electrical resistivity tomography (ERT), mise-a-la-masse (MALM), electrical capacitance measurement (ECM), spectral induced polarization (SIP), earth impedance method (EIM), electrical impedance spectroscopy (EIS), and electrical impedance tomography (EIT)

across various species and growth conditions, are still needed to better understand high frequency polarization in roots.

Conduction is assessed by measuring the resistance and then calculating resistivity or conductivity, whereas polarization is assessed by measuring the capacitance of the biological tissue. Both conduction and polarization can also be assessed simultaneously by measuring the electrical impedance of a biological tissue and then calculating effective material properties (complex resistivity or conductivity) by using a geometric factor *K,* which accounts for the geometric dimensions of the measurement (see the Glossary). In this case, the real part is associated with electrical conduction, whereas the imaginary part is associated with electrical polarization.

1.2 | Overview of electrical methods for root system investigation

These methods target either electrical resistance, capacitance, or impedance and are classified into eight categories, in order of appearance in the following sections: electrical resistance measurements (ERM), ERT, mise-a-la-masse (MALM), electrical capacitance measurements (ECM), earth impedance method (EIM), EIS, spectral induced polarization (SIP), and electrical impedance tomography (EIT). Some of these methods share the same physical principles, but they differ in their application scale (root scale, plant scale, and plot scale), the frequency of the electric field (e.g., single frequency or multiple frequencies), and the amount and position of electrodes, as illustrated in Figure 2.

Methods at the root and plant scales have mainly been used in fundamental studies or to obtain information on key parameters that can be used to interpret results from measurements at the field scale. They are also useful to determine if sufficient contrast in the electrical signature can be expected in field measurements. In this review, we will give an overview of these different measurement techniques coming from various scientific communities and will discuss their functioning and potential for root system investigation.

2 | METHODS TARGETING ELECTRICAL RESISTIVITY

2.1 | ERM

Some studies have used relatively simple ERM to investigate plant roots (Anderson & Higinbotham, 1976; Cao, Repo, Silvennoinen, Lehto, & Pelkonen, 2010). An ERM setup consists of a multimeter and two electrodes connected along a

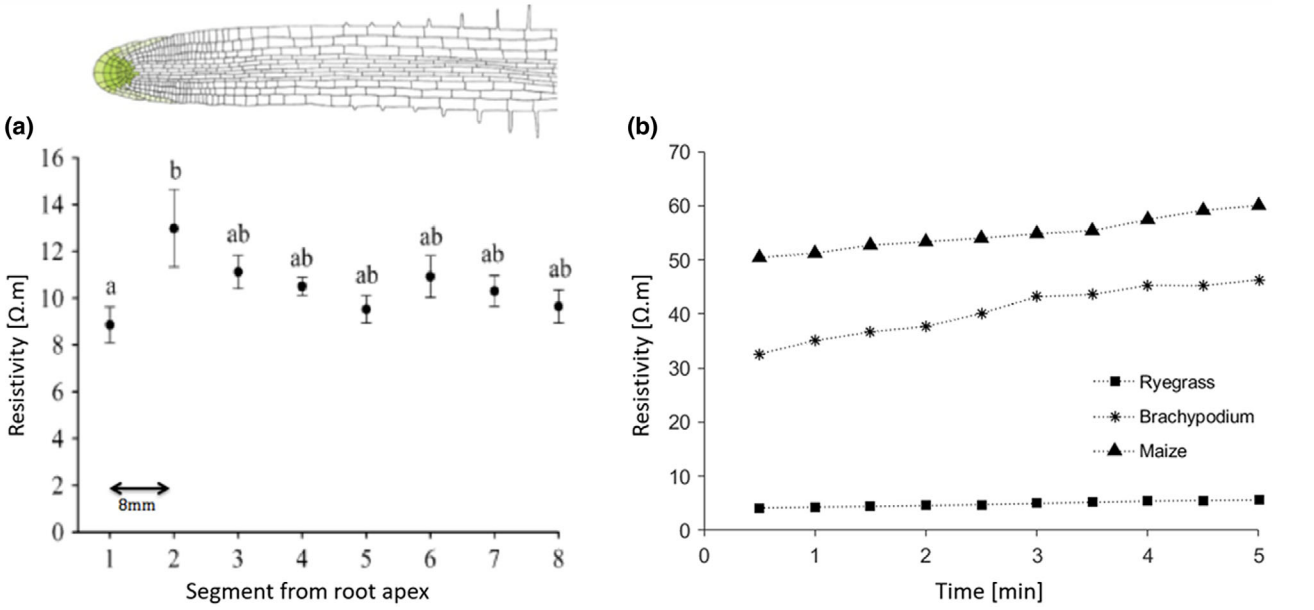

FIGURE 3 Application of electrical resistance measurement (ERM) for root studies. (a) Resistivity variation along a segment of willow roots, segments with same letter code show no significant difference (Reproduced from Cao et al., 2010, with permission of Oxford University Press). (b) Resistivity variation across species (Ehosioke et al., 2017)

single root segment (root scale) or with one electrode in the plant stem and the second one in the growth medium (soil and hydroponics; plant scale). The electrodes are simultaneously used for current injection and potential measurements. The main output of such measurements is the electrical resistance or resistivity of the studied system provided that an appropriate geometrical factor can be identified. The experimental setup is simple and typically operates at the centimeter scale. The understanding of the electrical response of single root segments is important since it is a first step towards discriminating root electrical signals from those of other soil properties and state variables, especially in combination with modeling (Rao et al., 2019).

Anderson and Higinbotham (1976) pioneered the study of electrical resistance of root segments by measuring longitudinal electrical resistance along 2-cm segments of maize (*Zea mays* L.) roots cut at varying distances from the root apex. The older root segments further away from the apex had a greater electrical resistance than the younger segments, except for the section just before the apex, which showed the greatest resistance. They attributed this to the proportionately large number of cells in the meristem and in the early stages of the elongation zone. However, only the resistance was measured, and the corresponding root diameters were not reported. Therefore, it is not possible to discriminate possible geometrical factors (i.e., differences in root diameter) from inherent electrical root properties, which compromises the interpretation of these measurements.

Cao et al. (2010) used ERM in a hydroponic system to study root morphology and the variation of axial resistivity along a single root segment of willow (*Salix schwerinii* E. Wolf). They calculated axial resistivity at varying distances from the apex (Figure 3a). They found the highest resistivity just before the root tip and observed a gradual reduction in resistivity towards the root collar. The high axial resistivity next to the root tip was attributed to the presence of a hydraulically isolated segment with immature metaxylem and mature protoxylem (Frensch & Steudle, 1989). The root tip itself showed the lowest resistivity, which was attributed to underdeveloped cell walls with a very permeable membrane that allow fast movement of solute and water between the root tip and soil (Frensch & Steudle, 1989).

Cao et al. (2010) also measured the resistance of the stem–root system at different immersion depths of the root system in a hydroponic solution. Afterwards, the roots were cut off and the resistance of the stem was measured. The excised roots were scanned to assess the surface area, and the number of lateral roots was obtained using image analysis (WinRhizo). They found that the measured resistance correlated significantly with root surface area (r^2 = .75) and the root length (r^2 = .63), which is expected and linked to the geometric factor, and to a lesser extent with the number of lateral roots (r^2 = .56). This suggests that ERM could be useful to study root morphology. The submerged part of the root system played a negligible role, which is probably due to current leakage at the stem–solution interface. They also found that the average resistivity of the roots (10.5 Ωm) was much smaller than that of the stem (108.3 Ωm), which was attributed to the anatomical differences between the root and stem. For example, the vascular tissue is thicker and more

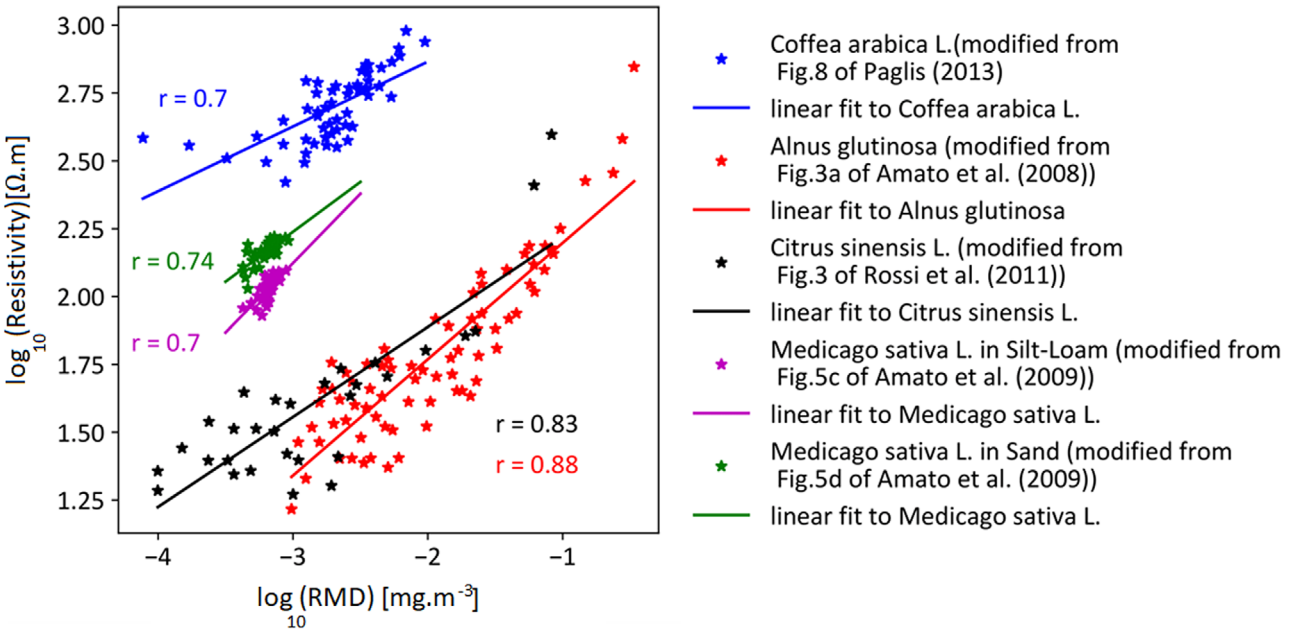

FIGURE 4 Root mass density (RMD) vs. electrical resistivity (ρ) of various plant and tree species derived from different studies as described in the legend, *r* is the correlation coefficient. Digitization of pictorial data done using WebPlotDigitizer (Rohatgi, 2011)

developed in stems than in roots (Longui, Romeiro, & Alves, 2012).

Recently, Ehosioke et al. (2017) used ERM measurements to determine the electrical resistivity of root segments of three different plant species: maize, ryegrass (*Lolium perenne* L.), and *Brachypodium*. Their results showed that electrical resistivity of roots varied for different species (Figure 3b). It was found that the variation in electrical resistivity could be linked to the structural variation and anatomical differences between the species.

A major limitation of ERM is that it is hard to obtain knowledge on the structures that are contributing most to the electrical conduction. In addition, roots were excised before ERM measurements in some studies (Anderson & Higinbotham, 1976; Cao et al., 2010). In this case, the cut surface in contact with the nutrient solution may introduce a bias because of an increased absorbing surface area.

2.2 | ERT

Electrical resistivity tomography, also called DC resistivity imaging (DCR) or electrical resistivity imaging (ERI), determines the distribution of electrical resistivity by performing a set of resistance measurements on the ground surface and/or in boreholes. Measurements are performed by injecting current via two electrodes, and the resulting voltage difference is measured at two other electrodes using various combinations of current and potential electrodes along a transect or grid. In order to determine the resistivity of the subsurface, a geophysical inversion of the measured resistances must be performed. The obtained resistivity distributions are typically presented as tomograms. Since the inverse problem is ill posed, the obtained resistivity model is nonunique and typically represents a smoothed representation of the actual resistivity distribution.

Electrical resistivity tomography is interesting for root system investigations because of its high two- or three-dimensional spatial coverage, acquisition speed, minimally invasive nature, and cost effectiveness. Some ERT studies focused on root biomass estimation, whereas others focused on physiological processes such as water and nutrient uptake by the root system, but these are mainly interpretation perspectives rather than a prior methodological difference, as both aspects can be captured by time-lapse ERT measurements.

Figure 4 compares results from several studies that have directly correlated bulk resistivity with root biomass with varying success (Amato et al., 2008, 2009; Rossi et al., 2011; Paglis, 2013). Bulk soil resistivity is known to be strongly influenced by soil moisture content, porosity, mineralogy, temperature, and salinity level and only to a lesser extent by roots. Thus, the contrast between roots and soil depends highly on soil type and saturation state (Rao et al., 2019) and is therefore varying with time. In addition, fine roots actively take up water and nutrients and release different exudates. These processes also affect resistivity at several temporal scales, ranging from daily (night vs. day, sunny vs. cloudy days) to seasonal (growth period vs. winter or drought season)

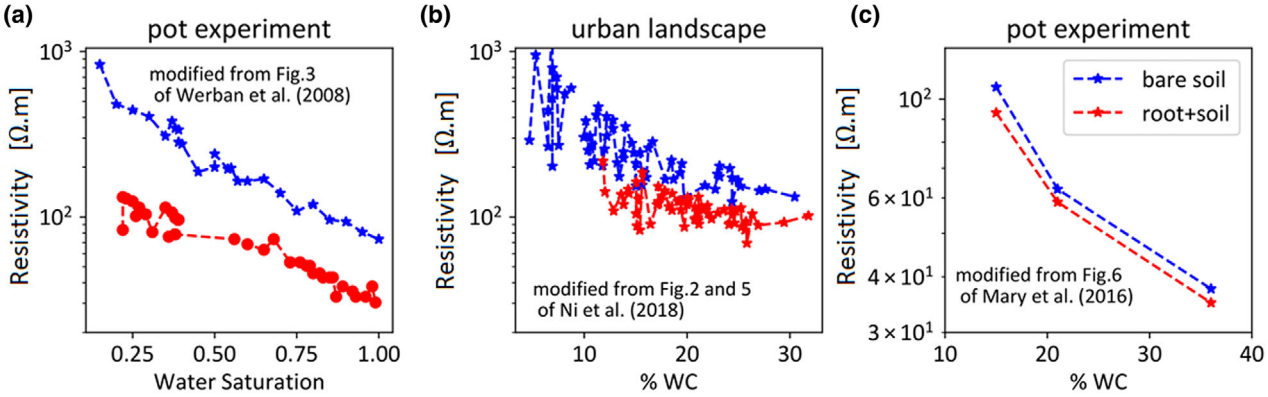

FIGURE 5 (a) Electrical resistivity (ρ) vs. water saturation from Figure 3 of Werban et al. (2008). (b) Electrical resistivity (ρ) vs. percentage volumetric water content (WC) from Figure 2 and Figure 5 of Ni et al. (2018). (c) Frequency averaged resistivity magnitude (|ρ|) as a function of percentage volumetric water content of Mary et al. (2016)

variations (Mary et al., 2018). Based on these considerations, it is clear that the relationships shown in Figure 4 are site specific and without generality. Overall, ERT may lack direct sensitivity to root properties due to the variations in the contrast between bulk soil and root electrical resistivity and the relatively low volume fraction of roots. Using resistivity as a predictor for root biomass without taking these factors into account is therefore highly uncertain (Rao, Lesparre, Orozco, Wagner, & Javaux, 2020).

Electrical resistivity tomography has also been used to investigate physiological processes such as water and nutrient uptake, which is promising given the high sensitivity to water content in the root zone. A range of studies have reported areas of contrasting resistivity (in time and space) that were attributed to root water uptake processes beneath herbaceous plants (Beff et al., 2013; Garré, Günther, Diels, & Vanderborght, 2012; Michot et al., 2003; Moreno, Arnon-zur, & Furman, 2015; Panissod, Michot, Benderitter, & Tabbagh, 2001), and some shrubs and trees (Hagrey, Meissner, Werban, Rabbel, & Ismaeil, 2004; Hagrey & Michaelson, 2002; Jayawickreme, Van Dam, & Hyndman, 2010; Katul, Todd, Pataki, Kabala, & Oren, 1997; Koumanov, Hopmans, & Schwankl, 2006; Robinson, Slater, & Schäfer, 2012). Electrical resistivity tomography has also been used in orchards to study soil moisture dynamics and irrigation patterns near cash crops such as fruit trees (Lazzari et al., 2008; Loperte et al., 2006). These studies found an increasing resistivity in the root zone due to drying through root water uptake processes, but some root zones show lower resistivity than the background as shown in Figure 5 (Lazzari et al., 2008; Petersen & Al Hagrey, 2009; Rodríguez-Robles, Arredondo, Huber-Sannwald, Ramos-Leal, & Yépez, 2017; Werban, Attia al Hagrey, & Rabbel, 2008). The low resistivity of fine roots and high resistivity of tree roots reported in the studies discussed above is an indication that roots are a contributing factor, although masked by other factors, as discussed above. The effect of root biomass can only be clearly distinguished with additional independent measurements.

Many examples exist where time-lapse ERT has been used to quantify water and solute fluxes in a range of agricultural systems, including maize (Beff et al., 2013; Michot et al., 2003), barley (*Hordeum vulgare* L. ; Garré et al., 2011), mixed cropping (Garré et al., 2013), and orchards (Cassiani et al., 2015; Moreno et al., 2015; Vanella et al., 2018). Interestingly, none of these studies accounted for the potential effect of root biomass on the measured resistivity. This is most probably because the sensitivity of ERT to soil moisture is larger than to root biomass in most cases, especially when looking at time-lapse differences. Nevertheless, Rao et al. (2019) already warned that this might not always be the case. Using coupled electrical and root water uptake models, they showed that the bias in soil moisture estimates may be up to 50% when roots are not properly accounted for. Although ERT is less sensitive to roots than other system properties (soil texture, porosity, stone fraction, mineralogy) and state variables (soil temperature, fluid conductivity, soil moisture), the influence of roots can be consistent. Therefore, there is a need for auxiliary data to separate root effects from other properties and variables.

2.3 | MALM method

In the MALM method (Parasnis, 1967), an electric current is injected into a conductive body and the resulting voltage is measured at the ground surface located at certain distances around the body. The resulting voltage contours are then used to delineate the extent of the conductive body. In root studies, the conductive body is the plant stem–root system. This setup is based on the assumption that the current injected into a tree stem will be released into the soil through the root system, but only at the root–soil interface where roots absorb water and minerals from the soil.

Mary et al. (2018) used the MALM method jointly with ERT to characterize vine plant root water uptake at the plant scale. They injected current directly into the tree stem in one experiment and directly into the soil close to the stem in another experiment. It was observed that current injection into the stem produced very different voltage distributions in the soil compared with an injection into the soil. They concluded that current injected into the stem is redistributed in the soil by the root network. In a follow-up study, Mary, Vanella, Consoli, and Cassiani (2019) used MALM and ERT measurements to assess the root extent of citrus trees in an orchard under two different irrigation regimes (full and partial irrigation). The MALM measurements were used to map the locations of the active roots, whereas ERT was used to obtain quantitative information about the uptake of water by the roots. It was reported that the distribution of current flow for a stem injection was much different from that of a current injection into the soil in the case of partial irrigation. In contrast, no differences were observed in the case of full irrigation. This difference in behavior was attributed to differences in the resistivity contrast in the two cases. For partial irrigation, roots are likely more conductive than the surrounding soil, and the current flows preferentially through the roots. In the case of full irrigation, the surrounding soil is more conductive than the root, and the current is expected to leave the root system near the stem–soil interface, as also suggested by Urban, Bequet, and Mainiero (2011) and Peruzzo et al. (2020). Thus, the success of the MALM method depends on the contrast between the electrical properties of the root and that of the soil and on the contact resistance at the interface between the two. More studies are required to better understand root electrical properties, which are essential to improve the interpretation of MALM measurements.

2.4 | Measurements focusing on electrical capacitance

2.4.1 | ECM on single plants in soil

Electrical capacitance measurements are commonly used to study root systems at the plant scale (Chloupek, 1972; Dalton, 1995). Root capacitance is measured with an LCR meter (i.e., equipment that measures inductance, capacitance, and resistance of an electronic component) and two electrodes. One electrode is inserted into the stem, while the other is inserted into the growing medium. The capacitance is the amount of electric charge stored by the root system for a given electric potential (in farads). It quantifies polarization processes (stored charges) taking place in the root tissue upon current flow (Dalton, 1995; Rajkai, Végh, & Nacsa, 2002; Repo, Zhang, Ryyppö, & Rikala, 2000). Table 3 summarizes ECM applications reviewed below according to their target plant property: root biomass, morphology, or physiology.

We reviewed 138 studies that reported correlations between the measured capacitance (C_{root}) and root dry mass (R_{dm}), whereas another 14 studies reported correlations between C_{root} and root fresh mass (R_{fm}). The average correlation between C_{root} and R_{dm} was .77, whereas the average correlation between C_{root} and R_{fm} was .74. This suggests that ECM may be suitable for root biomass determination (see Figure 6). However, the range of correlation coefficients reported for R_{dm} (.30–.98) and R_{fm} (.51–.94) is large. This is due to other factors besides root mass that affect root capacitance, such as plant species (Aulen & Shipley, 2012), genotypes (Mcbride, Candido, & Ferguson, 2008), growing medium (Cseresnyés et al., 2017), and soil water status (Cseresnyés et al., 2018).

Based on 14 studies relating ECM to root morphology, there appears to be a correlation between C_{root} and root length or root surface area, with correlation coefficients ranging from .56 to .94 (average $R = .79$). Ellis, Murray, and Kavalieris (2013) tested the use of a four-electrode setup for ECM, which eliminated the high contact resistance present in the classical two-electrode setup. They observed very low correlations of C_{root} with root mass, area, and length ($R = .21$–$.31$). It was therefore concluded that electrical capacitance was a poor predictor of root dimensions in their analysis. Since C_{root} depends on tissue density and thus the position of stem electrodes, the setup of Ellis, Murray, and Kavalieris (2013) involved two stem electrodes. In particular, the second stem electrode (a potential electrode) is closer to the soil surface and thus reduces the influence of tissue density. This might explain the poor correlation they observed.

Investigations of root development with time using ECM showed that there are important temporal variations in the measured capacitance (Cseresnyés et al., 2018; Cseresnyés, Rajkai, & Takács, 2016; Cseresnyés, Takács, Füzy, & Rajkai, 2014; Cseresnyés, Takács, Füzy, Végh, & Lehoczky, 2016; Dalton, 1995). Cseresnyés et al. (2014) found that root water uptake and C_{root} increased from the emergence of a seedling to the beginning of flowering and then decreased continuously during the fruit setting for cucumber (*Cucumis sativus* L.) and bean (*Phaseolus vulgaris* L.). Similarly, ECM presented in Cseresnyés et al. (2018) identified peak activity with a capacitance value of 96.4 nF at a period that coincided with the completion of flowering 92 d after sowing. Afterwards, the capacitance decreased to 6.3 nF at Day 161, which coincided with the phenological stage of senescence. Senescence is associated with suberization and cell death, which is assumed to result in a lower capacitance. Cseresnyés et al. (2018) argued that ECM is more reliable for the estimation of root activity than for the estimation of root mass, length, and surface area. We tend to agree with this argument because root activity is a contributing factor in root biomass and morphology assessment using ECM, since most of these

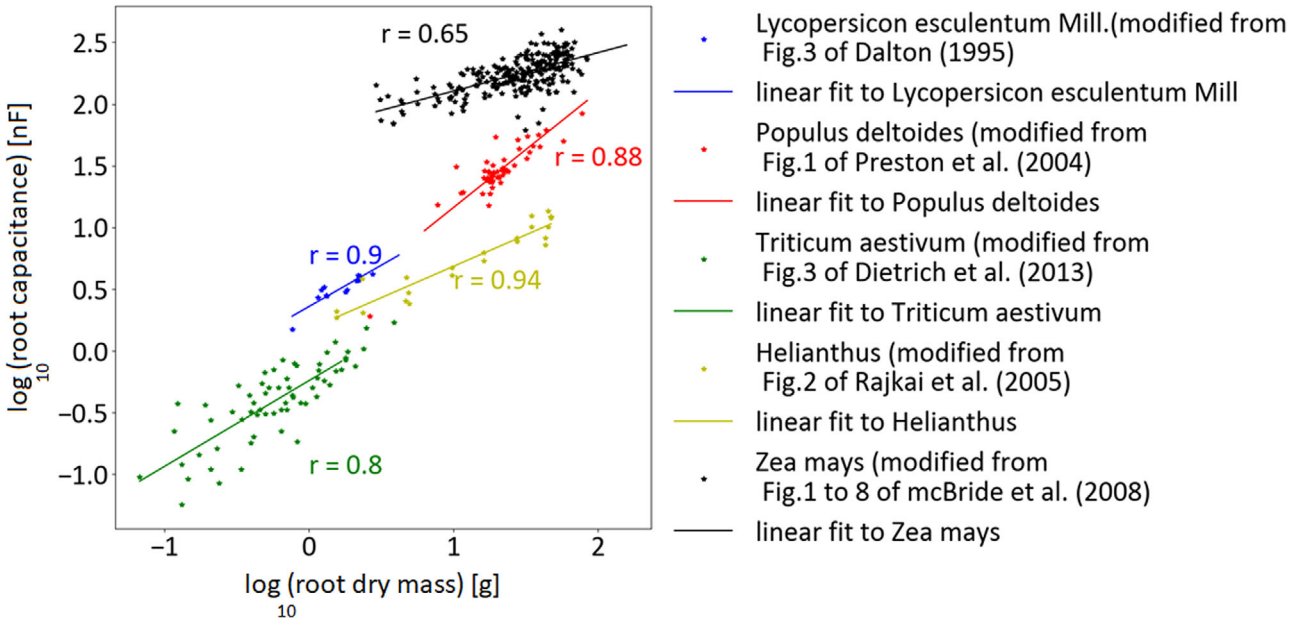

FIGURE 6 Log_{10} of Root dry mass (g) vs. log_{10} of electrical capacitance of roots (nF) of various plant and tree species taken from different studies as described in the legend. Digitization of pictorial data done using WebPlotDigitizer (Rohatgi, 2011)

measurements were performed on active plants. The large disparity among studies could be a reflection of the physiological state of the plant at the time of measurements.

Electrical capacitance measurements are usually performed using an LCR meter. Since capacitance is only clearly defined for an ideal capacitor, interpretation of the measured values relies on the selection of an appropriate equivalent circuit model. Dalton (1995) proposed a linear model assuming that roots behave as cylindrical capacitors and that their capacitances can be added together as if wired in parallel, suggesting that capacitance depends on the submerged root mass. Dietrich, Bengough, Jones, and White (2012) have shown that this model is too simplified and proposed an alternative equivalent circuit model (Figure 7) in which (a) the capacitance of the growth medium is much larger than the capacitance of the plant tissue, (b) the capacitances of tissues along an unbranched root can be considered as connected in series, (c) the capacitances of multiple unbranched roots comprising the whole root system act in parallel but reduce to the equivalent of a single capacitor, and (d) the capacitances of individual roots are directly proportional to their cross-sectional area or circumference. The model of Dietrich et al. (2012) indicates that the total capacitance is dominated by the aboveground part of the plant between the stem electrode and the growth medium. This may explain the wide range of results that have been obtained with ECM, since the distance between stem electrode and growth medium was not standardized in these studies.

An important point to realize is that soil water content affects capacitance measurements (a principle commonly used in the design of soil moisture sensors). However, ECM cannot distinguish the plant from the soil response. Many studies have circumvented this problem by making ECM on plants grown in hydroponic conditions. In situ monitoring of root activity may be feasible for ECM, but only under controlled conditions and after careful calibration. Such calibration is required, since capacitance is known to be influenced by species (Aulen & Shipley, 2012), genotypes (Mcbride et al., 2008), tissue density (Ellis, Murray, & Kavalieris, 2013; Ellis, Murray, et al., 2013), electrode type (Kormanek, Głąb, & Klimek-Kopyra, 2016), and growing media (Cseresnyés et al., 2017).

2.5 | Electrical impedance as a comprehensive target property

2.5.1 | EIM for single plants in soil

The EIM has been used to study physiological characteristics of root systems in situ, such as the absorbing root surface area (ARSA, Table 2). The setup relies on four electrodes, two current electrodes C_1 and C_2 for current injection, and two potential electrodes P_1 and P_2 to measure the resulting voltage. The current electrode C_1 is hammered into the stem, whereas C_2 is placed into the soil at a distance of about 10–20 m from the stem (depending on the tree size). The potential electrode P_1 is fixed into the root collar, whereas P_2 is inserted into the soil and moved repeatedly along the line connecting C_1 and C_2 (see Figure 8a). The measurements are used to calculate the grounding impedance I_g and to estimate ARSA (Aubrecht, Stanek, & Koller, 2006; Čermák, Ulrich, Stanek, Koller, &

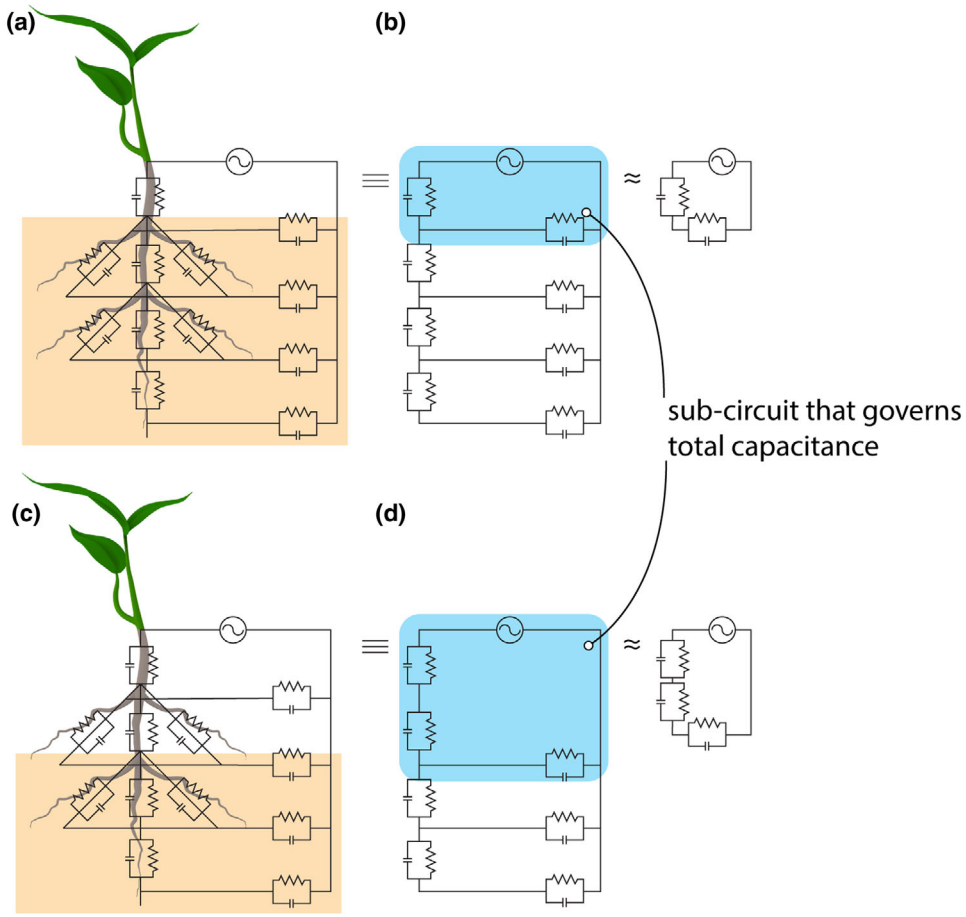

FIGURE 7 Resistance–capacitance (RC) circuits according to the Dietrich model. (a, c) Diagrams of barley plants with five root tips; (b, d) electrical equivalent networks of the root systems showing the location of the RC components. (a, b) The RC circuits for a completely submerged root system; (c, d) RC circuits for a partly submerged root system. The subcircuit that largely determines the capacitance is highlighted in blue to emphasize its importance. Note that the individual RC components can have different values. (reproduced from Dietrich et al., 2012, with permission from Oxford University Press)

Aubrecht, 2006) using

$$\mathrm{ARSA} = \rho \frac{L_{\mathrm{eff}}}{I_{\mathrm{g}}} \tag{1}$$

Where I_{g} is the grounding impedance, L_{eff} is the distance to the stem, and ρ is the wood resistivity. The wood resistivity is measured with two or four electrodes (depending on the tree size) while assuming that the tree is a cylinder (Aubrecht et al., 2006).

Aubrecht et al. (2006) described the theoretical basis of the EIM. The applicability of this method is based on the following crucial assumptions: (a) the xylem resistance is negligible and is not considered in the calculation of ARSA, (b) there is no radial conduction in woody or suberized root, which implies that electrical current is expected to flow through the entire root system and exit via the fine absorbing roots, (c) every absorptive part of a root branch is expected to contribute equally to the overall conductance, (d) root branches are expected to be electrically discrete resistors and tree root segments to be measured separately, (e) the ARSA is predominantly determined by the contact impedance between the root and the soil, and finally, (f) the soil impedance is a negligible part of the grounding impedance of a tree. Urban et al. (2011) assessed the applicability of the EIM to investigate tree root systems by testing these assumptions in several experiments, but they could not confirm that the assumptions listed above apply. Instead, their results clearly showed that a tree–root–soil continuum is a serial circuit where the xylem and soil impedance dominate the contact impedance. In particular, they showed that xylem electrical resistance is an important component of I_{g} and that I_{g} increases significantly with diameter at breast height (DBH) (Figure 8b). Therefore, the observed relationships between ARSA and DBH were site and soil specific. They concluded that the EIM cannot reliably assess the ARSA of distal fine roots because most of the charge carriers exit the root system in the proximal parts of the root–soil interface. Čermák et al. (2013) compared

TABLE 2 Summary of the relationship between low-frequency electrical methods and root properties based on the existing application of the reviewed methods

Method[a]	Application category	Specific root property
ERM	Morphology	Surface area, length, and number of lateral roots
	Anatomy	Structural variation along a single segment
ECM	Biomass estimation	Dry mass and fresh mass
	Morphology	Length and surface area
	Physiology	Root activity (water and nutrient uptake)
EIM	Physiology	Absorbing surface area (root absorptive index)
MALM	Physiology	Location of active roots
EIS/SIP	Anatomy	Structural change in roots with age
	Morphology	Surface area and root system size
	Physiology	Growth monitoring, mycorrhizal colonization, cold acclimation, and health state
	Biomass estimation	Resistivity and polarization contrast between root and soil
ERT	Biomass estimation	Root mass density
	Physiology	Water uptake
EIT	Anatomy	Structural change in roots
	Physiology	Root decay due to nutrient deprivation
	Biomass estimation	Resistivity and polarization contrast between root and soil
	Morphology	Root spatial extent

[a]ERM, electrical resistance measurements; ECM, electrical capacitance measurements; EIM, earth impedance method; MALM, mise-a-la-masse; EIS, electrical impedance spectroscopy; SIP, spectral induced polarization; ERT, electrical resistivity tomography; EIT, electrical impedance tomography.

results from the EIM with those obtained from scanning and microscopy of Norway spruce [*Picea abies* (L.) Karst.] at two different sites. The root absorptive index value obtained from EIM (0.7 m^2 m^{-2}) was the lowest for both sites compared with the 2.2 and 1.2 m^2 m^{-2} obtained for the scan and microscopy, respectively. This suggests that ARSA obtained by the EIM is not reliable and thus agrees with the conclusion of Urban et al. (2011). In the field, various determinants of soil and xylem resistivity exist: for example, soil texture and porosity (Chloupek, 1972), root density (Amato et al., 2008), moisture of the soil and xylem (Hagrey, 2007; Zenone et al., 2008), and also cell anatomy (van Beem, Smith, & Zobel, 1998; Zhang, Willison, & Willison, 1991). These factors vary in space and time, causing I_g and L_{eff} to vary independently of ARSA, which makes it difficult to determine ARSA from the EIM alone.

2.5.2 | The value of measurements at multiple frequencies

Measurements at multiple frequencies offer more potential for root investigation because the use of different frequencies allows to separate processes that have different time or spatial scales. Methods using multiple frequencies are classified here as EIS, SIP, and EIT.

2.5.3 | EIS and SIP

Electrical impedance spectroscopy determines the impedance of the soil–plant continuum across a range of frequencies (hertz to megahertz). This method has been used in many studies in plant science and medicine (Bera, Bera, et al., 2016; Bera, Nagaraju, & Lubineau, 2016; Coster, Chilcott, & Coster, 1996; Hayden, Moyse, Calder, Crawford, & Fensom, 1969; Inaba, Manabe, Tsuji, & Lwamuto, 1995; Klauke et al., 2005; Lin, Chen, & Chen, 2012; Macdonald, 1992; Shrivastava, Barde, Mishra, & Phadke, 2014a, 2014b). For root studies, EIS has been used to assess the morphological and physiological properties of roots such as root growth (Ozier-Lafontaine & Bajazet, 2005; Repo, Laukkanen, & Silvennoinen, 2005), estimation of root system size (Cao, Repo, Silvennoinen, Lehto, & Pelkonen, 2011), and mycorrhizal colonization of roots (Cseresnyés, Takács, Végh, Anton, & Rajkai, 2013; Repo, Korhonen, Laukkanen, Lehto, & Silvennoinen, 2014; Repo, Korhonen, Lehto, & Silvennoinen, 2016), as summarized in Table 4. An EIS setup consists of an impedance analyzer and two or three electrodes; one is typically inserted into the root collar, while the other(s) is fixed into the growth substrate. The electrode can be a stainless steel needle (Repo et al., 2014), a tension clamp (Cseresnyés, Takács, et al., 2013; Cseresnyés, Rajkai, & Vozáry, 2013),

TABLE 3 Summary of electrical capacitance measurement (ECM) applications

Reference	Plant species	Root properties	Correlation	Growth medium	Observations
Chloupek, 1972	*Zea mays*	Dry mass	.728	Sand	
	Helianthus annuus	Fresh mass	.692	Clay soil	
Chloupek, 1977	*Helianthus annuus*	Fresh mass	.54, .566	Sand	
	Daucus carota	Fresh mass	.514	Loam soil	
Kendall et al., 1982	*Trifolium pretense*	Dry mass	.672	Hydroponics	
	Medicago sativa	Dry mass	.50	Silt loam	
Dalton, 1995	*Solanum lycopersicum*	Dry mass	.77	Hydroponics	Linear relation
van Beem et al., 1998	*Zea mays*	Fresh mass	.73	Vermiculite	
	Zea mays	Fresh mass	.53	Loam (field)	
Preston, McBride, Bryan, & Candido, 2004	*Populus deltoids*	Fresh mass	.866	Potting soil	
Rajkai, Végh, & Nacsa, 2005	*Helianthus annuus*	Fresh mass	.832, .921	Sandy soil	Needle & clamp electrodes
Ozier-Lafontaine & Bajazet, 2005	*Solanum lycopersicum*	Dry mass	.987, .829	Hydroponics & clay loam	Linear and exponential relation
	Amaranthus tricolor	Fresh mass	.937		
Mcbride et al., 2008	*Zea mays* (inbreeds and hybrids)	Dry mass	.779, .647, .761, .823, .364, .846	Hydroponics + Turface	Different genotypes showed unique capacitance relation with dry mass
Bengough et al., 2009	*Triticum aestivum*	Dry mass	.753	Gravel–sand mix	
Tsukahara, Yamane, Yamaki, & Honjo, 2009	*Prunus persica*	Fresh mass	.897	Soil (field)	
	Prunus persica	Dry mass	.806	Soil (potsoil)	
Chloupek, Dostál, Středa, Psota, & Dvořáčková, 2010	*Daucus carota*	Fresh mass	.525	Soil (field)	
Pitre et al., 2010	*Salix viminalis*	Dry mass	.81	Soil (potsoil)	
	Salix schwerinii	Dry mass	.49	Sandy soil (field)	
Aulen & Shipley, 2012	Herbaceous species (10 different plants)	Dry mass	.30	Compost	Requires species-specific calibration, regression strength not strong
Dietrich et al., 2012	*Hordeum vulgare*	Fresh mass	.869	Hydroponics	No linear relation when roots were raised from solution
		C/s area	.806, .771		Proposed a new model in place of Dalton model
Dietrich, Bengough, Jones, & White, 2013	*Triticum aestivum*	Dry mass	.753	Sand	Confirmed the model proposed by Dietrich et al., 2012 EC measured in wet substrate ≠ direct assessment of root mass
Ellis, Murray, & Kavalieris 2013	*Vicia faba*	Root length	.56	Sand	EC is a poor predictor of root size and depends on tissue density
Ellis, Murray, et al., 2013	Various	Root length	.94	Moist clay-loam (plantation)	Position of stem electrode affected EC values

(Continues)

TABLE 3 (Continued)

Reference	Plant species	Root properties	Correlation	Growth medium	Observations
Cseresnyés, Takács, et al., 2013	*Zea mays*	Dry mass Length Surface area	.9230 .9183 .9367	Pumice	Higher values and stronger correlation found in mycorrhiza-colonized roots
Postic & Doussan, 2016	*Triticum turgidum*	Dry mass	.787	Loam	Recommended more than two-electrode setup and clamp electrode for stem
Cseresnyés, Rajkai, & Takács, 2016	*Glycine max*	Dry mass	.844, .895, .936	Pumice	EC was affected by drought, EC increased with age (DAP), peaks during flowering and decreased after
Carlson & Smart, 2016	*Salix salicaceae*	Dry mass	.88	Peat moss	Root dry mass relationship with EC is strongly linked with stem dry weight
Kormanek et al., 2016	*Fagus sylvatica*	Dry mass	.502 (cylinder), .747 (rect. el.)	Loam (forest nursery)	Rectangular electrode correlated better with all parameters than cylindrical electrode
		Total root area	.641 (cylinder), .818 (rect. el.)		Proposed a two-dielectric model in place of Dalton model
		Total root length	.688 (cylinder), .802 (rect. el.)		
Cseresnyés, Takács, Füzy, Végh, & Lehoczky, 2016	*Zea mays A. theophrasti*	Dry mass	.901 .954	Arenosol	EC increased with age, with peaks around 27–31 DAP, and then decreased.
Cseresnyés et al., 2017	*Cucumis sativus*	Dry mass	.688	Arenosol	Capacitive effect of the growth media increased with the complexity of the substrate
		Length	.726		Correction for dissipation factor (capacitive effect) improved correlation
		Surface area	.683		
	Triticum aestivum	Dry mass	.879	Pumice	
		Length	.866		
		Surface area	.897		
Cseresnyés et al., 2018	*Zea mays*	Dry mass	.882–.911	Chernozem soil	Root activity increased until flowering and decreased during maturity
	Glycine max		.831–.874		

Note. C/s, cross-section; EC, electrical conductivity; DAP, days after planting; rect. el., rectangular electrode.

or a nonpolarizable Ag/AgCl electrode (Ozier-lafontaine & Bajazet, 2005).

Macdonald (1987) describedvvvv two distinct ways to analyze the impedance spectra of a particular system. At a macroscopic level, the impedance spectra of the system can be analyzed using equivalent circuit models. Alternatively, interpretation can be done at a microscopic level by analyzing the impedance spectra in terms of the physicochemical properties of the system. Whereas the analysis of root impedance spectra at the microscopic level is still developing, equivalent circuit models are commonly fitted to impedance spectra measured on roots.

There are two types of equivalent electric circuit models that have been commonly used to describe plant tissue: (a) distributed models that consist of distributed circuit elements (DCE) where a mathematical expression is used to describe the complex impedance (Repo, Zhang, Ryyppö, Vapaavuori, & Sutinen, 1994; Repo et al., 2005), and (b) lumped models that consist of a few ideal resistors and capacitors (Cole, 1940; Hayden et al., 1969; Inaba et al., 1995;

TABLE 4 Summary of electrical impedance spectroscopy (EIS) case application

References	Focus	Plant species	Setup	Growth media	Observations	Comments
Repo et al., 2005	Measurement of tree root growth	*Salix myrsinifolia* (willows)	40 Hz–340 kHz, two electrodes, silver needle for stem contact	Hydroponics	Sum of the resistors in the distributed model decreased with increasing root mass but was constant when the increase stopped	Could not differentiate the influences of the root mass, root surface area, and stem
Ozier-Lafontaine & Bajazet, 2005	Analysis of root growth	*Lycopersicum esculentum* (tomato)	10 Hz–1 MHz, two electrodes, Ag/AgCl for stem contact	Potsoil	Change in stem electrode position produced large variation in the IS, IS varied with plant age (DAP) in terms of Z', Z", and phase; their amplitudes decreased with root development (age)	Could not link the variations in IS with changes at soil–root interface or root internal medium during growth
Cao et al., 2011	Estimation of root system size	*Salix schwerinii* (willows)	60 Hz–60 kHz 2 electrodes, silver needle for stem contact	Hydroponics	The root–solution interfacial EC correlated linearly with the contact area of roots in solution for both "root and stem" and "root" (R^2 = .61)	Effect of stem was found to be stronger than the effect of roots; the dominating effect of stem needs to be verified by more studies using seed grown plants
Cseresnyés, Takács, et al., 2013	Mycorrhizal colonization of roots	*Zea mays* (maize)	100 Hz–10 kHz, two electrodes; tension clamp for stem contact	Pumice	Mycorrhizal plants showed slightly lower impedance than the nonmycorrhizal plants; EI showed a negative log relation with root dry mass, length, and surface area (R^2 = .8223–.9740); mycorrhizas increased root absorption surface area	Certain field conditions favor the use of EIS, whereas others favor the use of ECM; the impact of the growth medium on the result is not fully understood
Cseresnyés, Rajkai, & Vozáry, 2013	Impact of phase angle on EIS of roots	*Zea mays* (maize)	100 H–10 kHz, two electrodes, tension clamp for stem contact	Arenosol	Negative log relation was found between impedance and root extent parameters, dry mass (R^2 = .561 and .946) at 100 and 1,090 Hz, respectively; surface area (R^2 = .491 and .916) at 100 and 1,300 Hz respectively	Stronger correlations observed were linked to higher phase, plant age has remarkable effect on the phase

(Continues)

TABLE 4 (Continued)

References	Focus	Plant species	Setup	Growth media	Observations	Comments
Repo et al., 2014	Mycorrhizal colonization of roots (in situ)	*Pinus sylvestris* (Scots pine)	5 Hz–100 kHz, three electrodes, stainless needle for stem contact	Peat and vermiculite mixture	Cold acclimation and mycorrhizal colonization correlated with the IS (R^2 = .846)	Temperature affects EIS measurements on roots
Repo et al., 2016	Frost damage in mycorrhizal roots	*Pinus sylvestris* (Scots pine)	5 Hz–100 kHz, three electrodes, stainless needle for stem contact	Perlite with nutrient solution	Degree of cold induced injury increased with characteristic frequency, effect of freezing injury dominated that of mycorrhizal treatment	High IS variation was observed for roots of plants grown under similar conditions, the high IS variation might have been due to other external factors

Note. IS, impedance spectra; DAP, days after planting; Z', real part of impedance; Z'', imaginary part of impedance; EC, electrical capacitance; EI, electrical impedance; EIS, electrical impedance spectroscopy.

Zhang et al., 1991). Distributed models are used in cases where lumped models are not appropriate (e.g., highly differentiated tissues), since it may be necessary to match the measured spectra (Burr et al., 2001; Repo et al., 2005). However, it is challenging to formulate a circuit model that properly represents the root system and at the same time allows a physical interpretation of the model parameters (Repo et al., 2012). Typically, more than one equivalent circuit fits well to the impedance data, but most likely only one of them will provide a reasonable representation of the physical properties of the system (Ozier-Lafontaine & Bajazet, 2005; Repo et al., 2012; Srinivas, Sarah, & Suryanarayana, 2003). Current research therefore favors different interpretation methods such as principal component analysis (PCA) (Repo et al., 2014), Debye decomposition of the spectra (Weigand & Kemna, 2016), and fitting of impedance spectra using Cole–Cole models (Martin, Nordsiek, & Weller, 2015; Mary et al., 2017). Future studies should incorporate interpretations at the microscopic level based on the physicochemical properties of roots to improve the understanding of the polarization mechanisms at the root segment scale.

Ozier-Lafontaine and Bajazet (2005) measured the impedance spectra of a tomato (*Solanum lycopersicum* L.) root system at different growth stages. They found that the magnitude of the real and imaginary parts of the impedance decreased as the root age increased (Figure 9). They showed that root growth results in variations in root electrical properties, but the reasons for such variations (e.g., variations of the soil–root interface or the root internal properties) remained unclear.

Repo et al. (2014) classified the impedance spectra (5 Hz–100 kHz) of the root system of Scots pine (*Pinus sylvestris* L.) with PCA to investigate whether root colonization with mycorrhizal fungi (*Hebeloma* sp. and *Suillus luteus*) could be detected in situ. On average, the correlation between the impedance spectra and mycorrhizal fungi showed 29 and 38.5% change for *Hebeloma* sp. and *Suillus luteus*, respectively. This makes sense as mycorrhizal colonization and mutualism between tree and mycorrhiza is known to improve nutrient uptake of trees (Simard, Jones, & Durall, 2003).

Spectral induced polarization is a variant of EIS that is mainly used in the geophysical community. It uses a broad range of frequencies from millihertz to tens of kilohertz and four electrodes to reduce the influence of contact resistances and to improve the accuracy of the complex impedance measurements (Zimmerman et al. 2008). Spectral induced polarization has been successfully applied in various biogeophysical investigations (Abdel Aal, Atekwana, Slater, & Atekwana, 2004; Abdel Aal, Slater, & Atekwana, 2006; Atekwana & Slater, 2009; Atekwana, Werkema, & Atekwana, 2006; Kessouri et al., 2019). Mary et al. (2017) studied isolated coarse roots (in the laboratory) and found that coarse roots showed higher resistivity and polarized differently compared with soil, suggesting that SIP is a promising tool for root studies. Ehosioke et al. (2018) designed a new setup that allows the application of SIP to assess the electrical response of a single root segment without the influence of the stem and growing media. They observed a very large polarization response (0.4–0.8 rad) from crop root segments with peaks occurring around ~10 kHz. This is linked to interfacial polarization as discussed above, but more studies are needed to better understand this. Ehosioke et al. (2018) also observed a low phase error of 0.06 rad due to the contact impedance, which is very small compared with the polarization response from roots. This new setup was used to compare the electrical properties of primary root, seminal root, brace root, and stem of a maize plant grown in sand tubes at 27 d after sowing. The

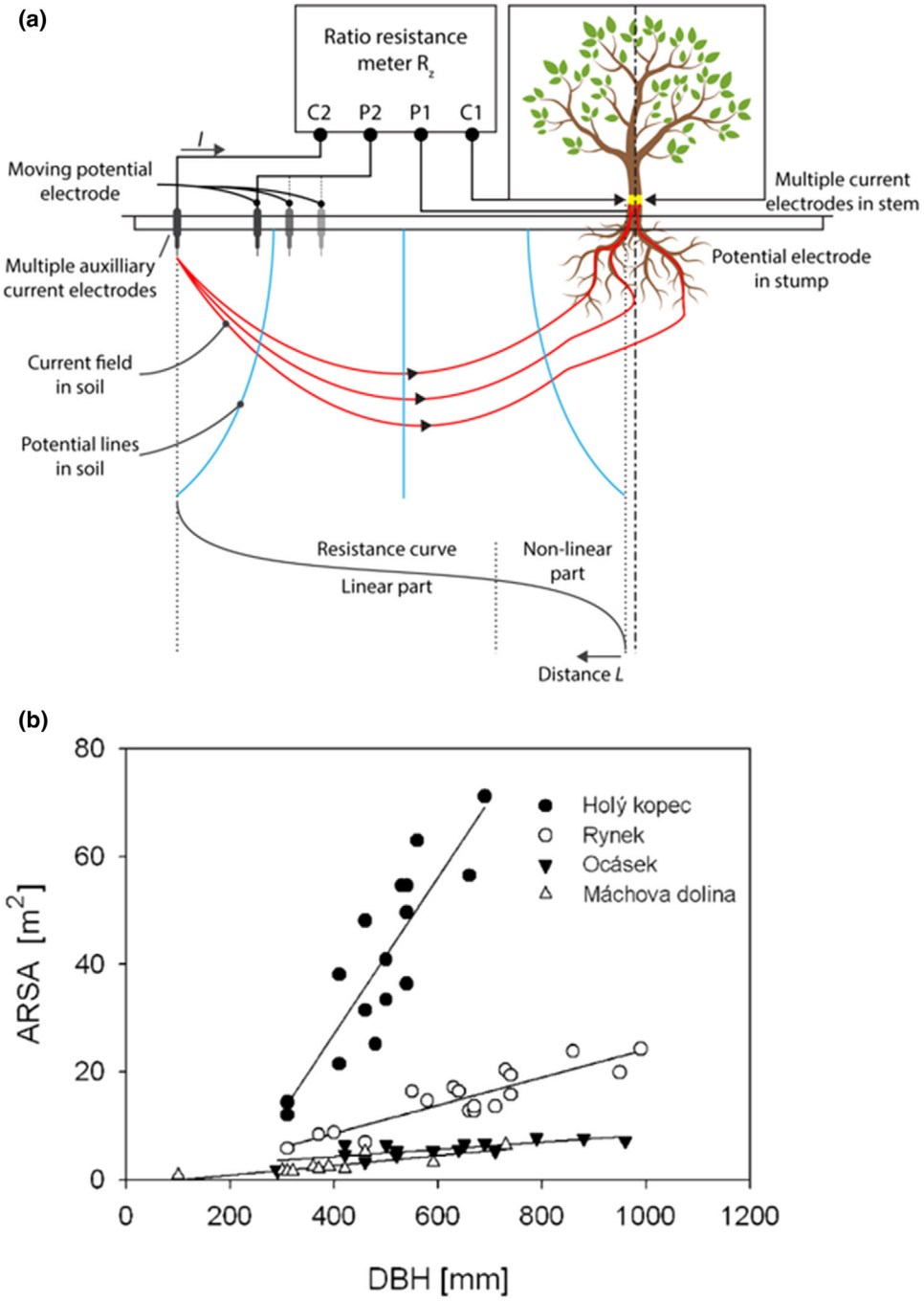

FIGURE 8 (a) Arrangement of the electrodes and an example of a resistance curve when potential electrode P2 is moved in a radial direction from the stem. (b) Relationship between the absorptive root surface area (ARSA) and the diameter at breast height (DBH) of European beech trees growing at four localities in the Czech Republic contrasting in soil conductivity. Site names in the legend are arranged according to soil conductivity with the latter increasing from Holy kopec to Machova dolina (right) (reproduced from Urban et al., 2011, with permission from Oxford University Press)

results show that the stem is more resistive than the root and displays a stronger polarization than the root (Figure 10). This implies that the plant stem and roots do not contribute equally to the electrical circuit of the stem–root–soil continuum. The stronger influence of the stem is probably due to the anatomical differences that exist between the root and the stem (Longui et al., 2012).

Recently, Tsukanov and Schwartz (2020) used SIP to investigate the relationship between the physical properties of wheat (*Triticum aestivum* L.) root grown in hydroponics and its electrical signature. They found a linear correlation between the electrical polarization in the 0.1 Hz to 1 kHz frequency range and root mass (r^2 = .97) and surface area (r^2 = .82). They also used SIP to monitor the electrical

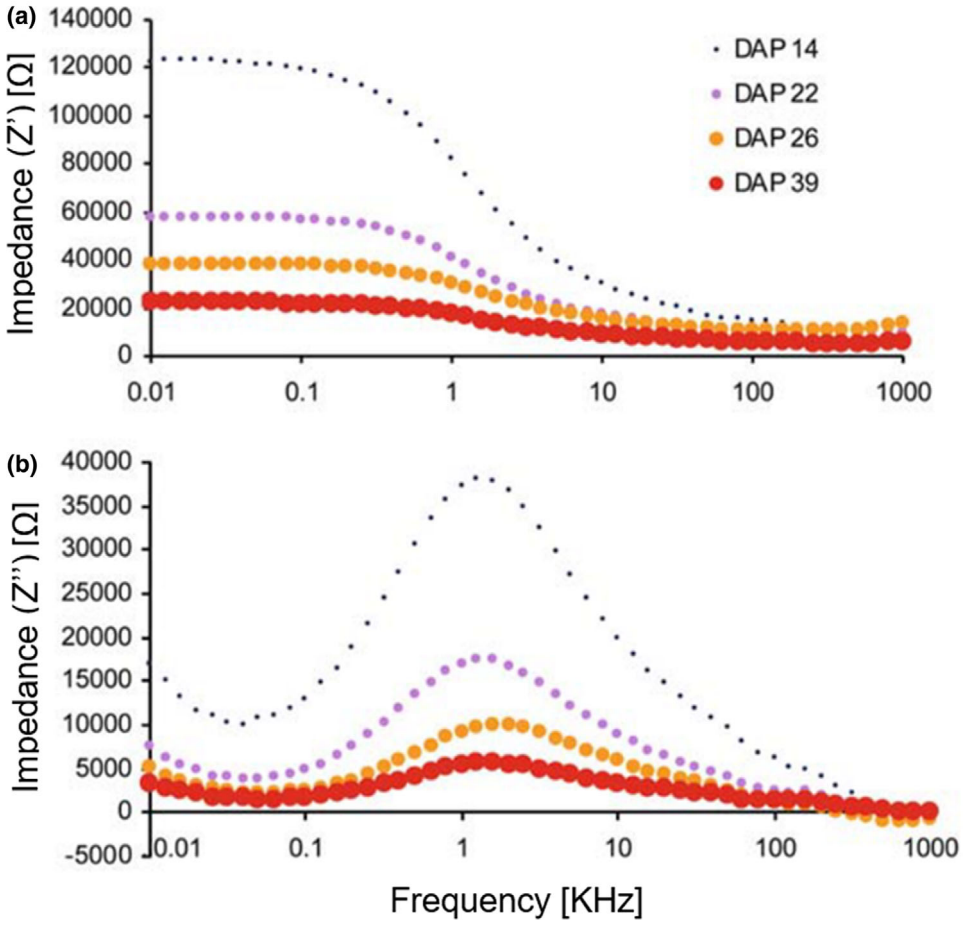

FIGURE 9 Electrical impedance spectra of tomato root systems: (a) real part (Z') of the impedance, (b) imaginary part (Z'') of the impedance, at different days after planting (DAP). The magnitude of the real and imaginary parts of the impedance decreased as the root age increased, which was linked to the increase in root system size with age (Figure 5 from reprinted Ozier-Lafontaine & Bajazet, 2005, reprinted with permission from Springer Nature)

response of wheat roots after poisoning the nutrient solution with cyanide. This led to a 30% decrease in polarization within 2 h. Their results further suggests that SIP is suitable to study morphology, physiology, and biomass of crop roots.

A key open challenge for EIS and SIP is the interpretation in the case of multicomponent systems. In geological systems, where the SIP method has been used widely and for decades, the physicochemical mechanisms of polarization for a single grain or pore throat are well understood, but the extrapolation of these mechanisms to a real porous media with heterogeneous characteristics (e.g., grain size, pore size, permeability, tortuosity, chemical heterogeneity, fluid phase distribution, etc.) is still a challenging task that requires theoretical developments (Kemna et al., 2012). Consequently, interpretation of complex impedance measurements in geosystems may be limited by the need to independently assess or assume the effects of chemical heterogeneity (Vaudelet, Revil, Schmutz, Franceschi, & Bégassat, 2011; Weller, Breede, Slater, & Nordsiek, 2011), temperature (Binley, Kruschwitz, Lesmes, & Kettridge, 2010; Martinez, Batzle, & Revil, 2012), saturation (Breede et al., 2012; Jougnot, Ghorbani, Revil, Leroy, & Cosenza, 2010), multiple fluid phases (Revil, Schmutz, & Batzle, 2011; Schmutz et al., 2010), grain size distribution (Revil & Florsch, 2010), pH (Skold, Revil, & Vaudelet, 2011), soil organic matter (Schwartz & Furman, 2015), or biological processes (Abdel Aal, Atekwana, & Atekwana, 2010; Atekwana & Slater, 2009; Ntarlagiannis, Williams, Slater, & Hubbard, 2005). In the particular case of root systems, interpretation of the complex impedance is difficult due to the complex architecture of roots and the inner root cell distribution and properties. Some setups involve the root–soil continuum, which adds the complexity of the geosystems to that of the root system with more variables to account for in the interpretation. Understanding of the root–soil–fluid interface from an electrochemical point of view and the inner root ionic distribution is necessary to properly interpret the overall signature when an external field is applied. More EIS and SIP studies at the root scale will help to improve the understanding of the main underlying mechanisms of polarization in roots, which is a

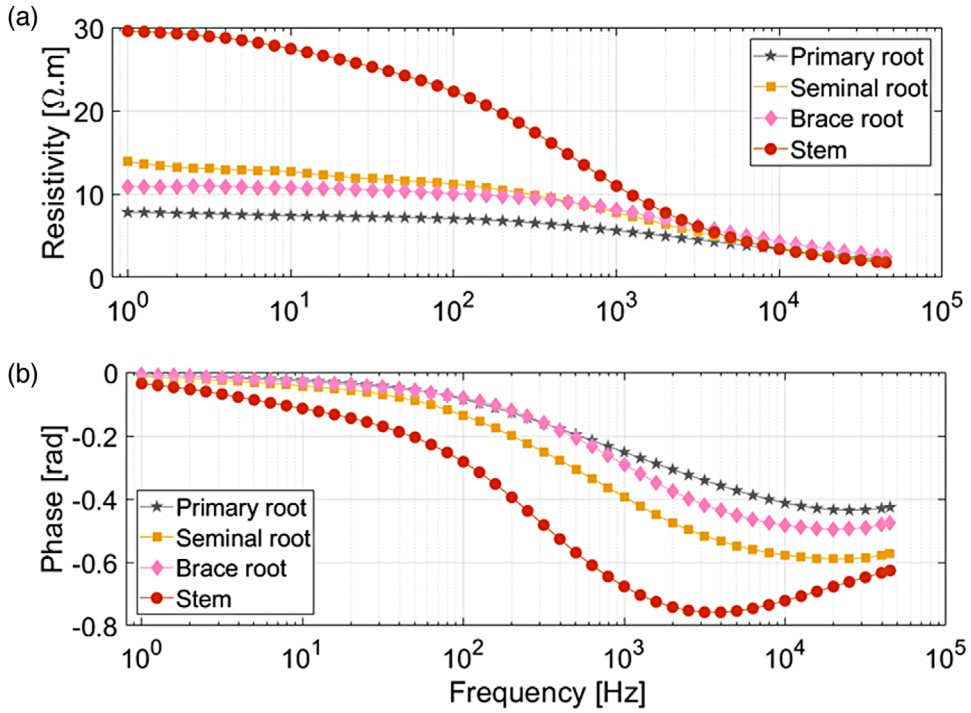

FIGURE 10 (a) Electrical resistivity and (b) phase spectra of primary root, seminal root, brace root, and stem of a maize plant at 27 d after sowing. The stem was found to be more resistive and polarizable compared with the root sections. This indicates that the contribution of the stem will dominate that of the roots when impedance measurements are made on a stem–root continuum

requirement for the development of a phytophysical model (Kessouri et al., 2019) that links root electrical signatures to root properties and root activity.

2.5.4 | EIT

Electrical impedance tomography is similar to ERT in terms of setup and measurement, but it uses a frequency-dependent current injection to determine the real and imaginary part (or amplitude and phase) of the complex impedance. Electrical impedance tomography is the imaging counterpart of SIP and has been used to obtain information about root system anatomy, physiology, and morphology, as well as for biomass estimation (Table 2). The advantage of this type of measurement over other geophysical methods is that it has the diagnostic advantages of spectroscopy and the spatial resolution benefits of a tomographic approach as described by Kemna et al. (2012).

Weigand and Kemna (2017) investigated the suitability of multifrequency EIT to characterize and monitor plant root systems in a laboratory rhizotron experiment. They monitored the spatiotemporal distribution of the complex electrical resistivity of the root system of an oilseed plant (*Brassica napus* L. subsp. *napus*) in a water-filled rhizotron under nutrient deprivation using EIT. Total polarization parameters obtained from the multifrequency EIT results showed a low-frequency polarization response of the root system (Figure 11), which enabled a successful delineation of the spatial extent of the root system. The magnitude of the overall polarization response decreased along with the physiological decay of the root system due to nutrient deprivation. The length scales (i.e., frequencies) at which polarization processes occurred also changed due to the prolonged nutrient deficiency.

Mary et al. (2016) investigated the suitability of EIT for mapping tree roots in dikes. They concluded that EIT is useful to interpret anomalies produced by woody roots. In a follow-up study, Mary et al. (2017) used EIT to map roots embedded in an actual soil and observed that the maximum phase contrast between root and soil occurred at a frequency of 1 Hz. Anisotropy in the polarization was also observed such that the polarization signal was strongest when the current lines were aligned with the root. Electrical impedance tomography seems promising for root system investigations. However, some challenges need to be addressed in its application in order to explore its full potential. Most laboratory studies are conducted in hydroponics or in homogeneous substrate, allowing good contrast to be obtained. In agricultural fields, however, the topsoil is heterogeneous due to grain size variations (resulting from weathering), presence of microorganisms (e.g., earthworms), and human activities such as plowing. Obtaining a good contrast for root system characterization in a heterogeneous agricultural field may be

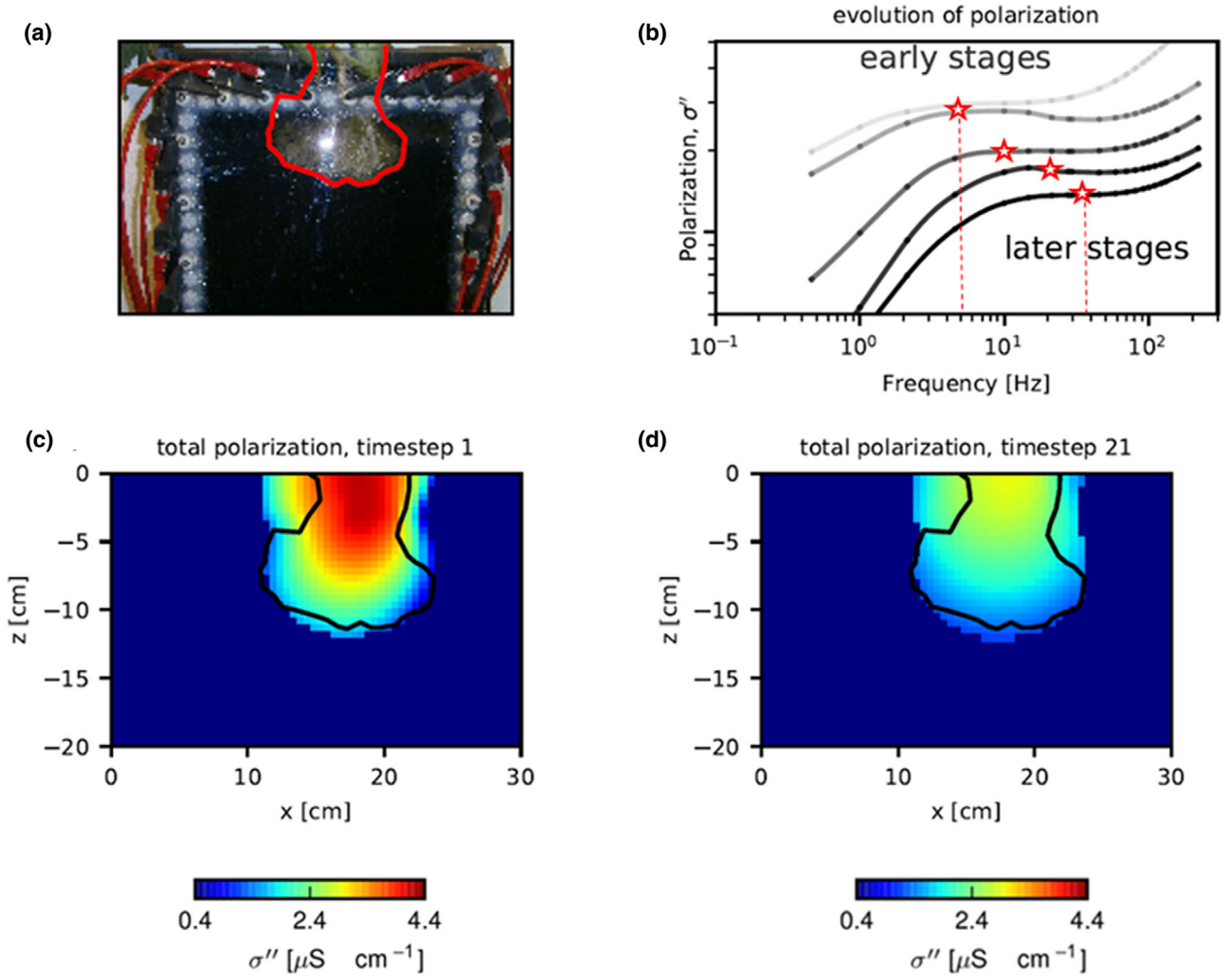

FIGURE 11 The spectral and spatial variation of polarization response of the root system of an oilseed plant: (a) the position of the bulk root system, and (b) the change in spectral shapes over time, showing decreasing polarization. The polarization occurred at a length scale indicated with dotted lines. (c, d) Spatial variation of the polarization response, showing (c) Time Step 1 and (d) Time Step 21. The change in spectral shape with time suggests that relaxation time distributions can provide additional information on the electrical response of root systems. The symbol σ'' is the imaginary conductivity; *z* and *x* are the vertical and horizontal dimensions of the rhizotron (modified from Weigand & Kemna, 2017, available under Creative Common Attribution 3.0)

difficult (Weigand, 2017). Other challenges are the acquisition of high quality data in the field due to noise and high electrode impedances (van Treeck, Zimmermann, Weigand, Huisman, & Kemna, 2017), forward modeling errors resulting from imprecise electrode locations, inaccurate discretization, and so on (Zhao et al., 2019). Upscaling laboratory observations to the field scale will require suitable measurement devices, experimental setups, and procedures adapted to field conditions.

2.5.5 | Joint discussion of stem injection methods

Measurement setups involving stem injection (Figure 2) of current as a means of characterizing root systems have commonly been used in a range of studies reviewed above. Although they adopted different methods such as ERM (Cao et al., 2010), ECM (Dietrich et al., 2012; Kendall, Pederson, & Hill, 1982), MALM (Mary et al., 2019; Peruzzo et al., 2020), EIM (Čermák et al. 2013; Urban et al., 2011), and EIS (Repo et al., 2005; Repo et al., 2012), it is interesting to note that all studies share a common conclusion. Proximal leakage of current at the stem–soil and solution interface appears as a common challenge in all measurement setups involving the stem–root–soil continuum. For example, Cao et al. (2010) observed that submerged roots did not contribute significantly to measured resistance, which is probably due to current leakage at the stem–solution interface. Urban et al. (2011) further supports this argument, as they concluded that distal roots conduct only a fraction of the current, and stem injection methods therefore cannot reliably estimate root system extent. Dietrich

et al. (2012) reported that excision of submerged roots did not affect capacitance and concluded that root capacitance is dominated by the tissue between the stem electrode and the solution interface, and closely related to the cross-sectional area of the root at the solution interface, thus agreeing with the findings of previous studies (Cao et al., 2010; Kendall et al., 1982; Repo et al., 2005; Repo et al., 2012; Urban et al., 2011). Mary et al. (2019) also observed proximal current leakage when the soil was wet and provided a more conductive pathway than the roots. Clearly, in situ applications of these methods should carefully consider other confounding variables, such as soil moisture (Cseresnyés et al., 2018; Mary et al., 2019), soil texture and porosity (Chloupek, 1972), tissue density (Ellis, Murray, & Kavalieris, 2013; Ellis, Murray, et al., 2013), electrode type (Kormanek et al., 2016), and growth media (Cseresnyés et al., 2017). In any case, careful calibrations will be required.

3 | SUMMARY AND CONCLUSIONS

3.1 | Resistance, capacitance, or impedance?

Plant scientists, earth scientists, and geophysicists all see potential in electrical methods to characterize the root system of plants given the observed correlations between electrical measurements or derived electrical properties with root biomass and/or root activity. Initial studies focused on resistance and capacitance measurements at a specific frequency, whereas recent studies have increasingly focused on impedance measurements at several frequencies; this approach allows both conduction and polarization effects to be studied simultaneously, giving information on roots at different time and spatial scales. Electrical conduction in bulk soil with roots is still mostly associated with soil moisture dynamics and is best used to study root physiological processes (e.g., soil water content changes associated with root water uptake). Electrical polarization of roots is related to the anatomy of the root tissue and cell structure (e.g., cell membrane properties), fluid composition, and plant metabolic state.

3.2 | Technical details of the measurement

Next to the targeted property, the technical details of the measurements (amount of electrodes, current injection strategy, electrode material, scale) determine the data quality and information content. In general, it was found that

- Four electrode measurements reduce problems with contact resistance and are therefore more reliable than measurements with two electrodes only.
- Injection schemes with an electrode in the stem (such as EIM, MALM, and EIS) are integrative measurements of the stem–root–soil continuum, and the results depend strongly on where the electrode is placed in the stem and the properties of the growing medium close to the stem, since the current may leave the system at the proximal parts of the root–soil interface.
- Multi-electrode schemes in the soil or a combination of injection in plant and in soil tend to give the most reliable and comparable results.

3.3 | Interpretation models

Equivalent electrical circuit models are essential to interpret contributions of different components in the soil–plant continuum governing electrical conduction and polarization during plant- or field-scale measurements. Small-scale measurements such as ERM and SIP on root segments (with or without the plant still connected) are important to validate equivalent electrical circuit models and to determine the contribution of individual components on the behavior of the full root architecture in the soil. Equivalent circuit models, however, are not very accurate because of the problem of nonuniqueness as more than one circuit model can provide a good fit for the impedance data. Therefore, there is an increasing use of alternative interpretation methods such as classification-based approaches (e.g., PCA), fitting of empirical spectral models (e.g., Cole–Cole model), or Debye decomposition of the spectra. Recent studies have shown that low-frequency polarization of root systems probably originates from polarization at various double layers, be it at cell membranes, or larger ion-selective structures such as the Casparian strip or the root surface. This is important not only to study roots, but also to study soil moisture and solute transport dynamics in relation to plant growth, since the contribution of the presence of roots to the measured electrical signal is now typically neglected. Interpretations at the microscopic level based on the physicochemical properties of the root should be incorporated to improve the understanding of the mechanisms driving polarization at root segment scale.

3.4 | Future research perspectives

More SIP studies should be used to understand the variability of root electrical properties in time and space, across species and genotypes. To achieve this, controlled experiments will be required to obtain fundamental information, and these experiments must be well designed and constrained to study the effects of each key parameter separately. Although different methods have investigated the influence of anatomy and physiological processes on the root electrical response, this is not yet fully understood. More studies are needed to link root anatomy and physiology with electrical properties

(conduction and polarization) of roots at different scales. Data obtained at root segment scale are necessary to validate phenomena underlying conduction and polarization occurring at the root segment and root architecture scale, and thus interpretation at the microscopic level will help to improve the understanding of the underlying mechanisms and establish models summarizing these phenomena.

Due to the complexity of the root system architecture embedded in the soil matrix, upscaling electrical properties measured at the root segment scale to plant scale or to field scale is a challenging task (Mary et al., 2016; Weigand & Kemna, 2017). Process-based multiscale numerical modeling of a soil–root continuum can thus pave a way for our understanding of upscaling mechanisms as we move from segment to plant and to field scale. A recent detailed numerical study at the plant scale shows that roots indeed affect ERT measurements and the effective electrical conductivity (Rao et al., 2019). However, explicitly representing root architecture (as in their study) in the computational domain demands a very high spatial resolution, thus increasing computational time and memory consumption. Further research on numerical approaches for such mechanistic models and the effect of the multiple scale levels involved in the underlying processes on the macroscopic properties is required. The parameterization of root segment electrical circuit models and how to link it to Cole–Cole or Debye decomposition models that will help interpret field measurements is also important.

4 | GLOSSARY

Alternating electric field: A voltage source in a medium usually produce an electric field that causes electric current to flow, if the medium is a conductor. If the electric charge (current) only flows in one direction, it is called direct current (DC). If the current changes direction periodically, it is known as alternating current (AC).

Capacitance (*C*): The electrical property of a capacitor that measures its ability to store an electrical charge on its two plates. The SI unit is farads (F).

Capacitors: These are devices that can store an electrical charge (current) when connected to a voltage source.

Cole–Cole model (CCM): A phenomenological model used to analyze SIP data. It is mostly used to describe the strength and frequency dependency of individual polarization peaks on SIP data. It is expressed as $\rho^* = \rho_\infty + (\rho_0 - \rho_\infty)/[1 + (\omega\tau)^c]$ where ρ_0 and ρ_∞ are low-frequency and high-frequency electrical resistivity values. respectively. $C = 1-\infty$, representing the CCM exponent that describes the relaxation time distribution. This can also be expressed in terms of complex conductivity (σ^*), but complex electrical resistivity is used often in practical terms because it is calculated directly from measured electrical impedance.

Current injection: The process of transmitting current through an object of interest to assess its electrical properties.

Debye decomposition: The process of determining a relaxation time distribution in place of a fixed number of relaxation time.

Polarization: In an electric field, electric charges do not flow through dielectric materials as they do in electrical conductors; instead, they shift from their equilibrium position, and the process is termed dielectric polarization. A dielectric material is an electrical insulator that can be polarized when an electric field is applied to it. Dielectric properties refer to the storage and dissipation of electric and magnetic energy in materials.

Dielectric relaxation: Momentary delay (lag) in the dielectric constant of a material. The dielectric constant is the measure of a material's ability to store electrical energy in an electric field.

Electrical impedance (*Z*), resistivity (ρ), and Conductivity (σ) (real, imaginary, magnitude, and phase): Electrical impedance is the measure of the opposition that a circuit offers to a current when a voltage is applied. Impedance represents the concept of resistance in AC circuits and has both magnitude and phase. In DC circuits, resistance could be expressed as impedance at zero phase angle. Impedance is a complex number, the SI unit is ohms (Ω), just like resistance. Impedance (Z) is defined in Cartesian form as $Z^*_{(w)} = Z'_{(w)} + jZ''_{(w)}$ where w is the angular frequency, j is the imaginary number, Z' is the real part (representing conduction), and the Z'' is the imaginary part (representing polarization).

Electrical resistivity (ρ) is an inherent property of a material that quantifies its opposition to the flow of electrical current. Its SI unit is ohm meters (Ω m). Electrical conductivity (σ) is a measure of materials ability to conduct electric current. The SI unit is siemens per meter (S m^{-1}). It is the reciprocal of electrical resistivity. Complex resistivity (ρ*) and conductivity (σ*), which are effective material properties, can be calculated from the impedance using a geometric factor K, which accounts for the geometric dimension of the measurement: $\rho^*_{(w)} = KZ^*_{(w)} = \rho'_{(w)} + j\rho''_{(w)} = |\rho|(\cos\varphi + j\sin\varphi) = |\rho|e^{j\varphi}$, where |ρ| is the resistivity magnitude, and ϕ is the phase shift. $\sigma^*_{(w)} = 1/\rho^*_{(w)} = 1/KZ^*_{(w)}$.

Electrode: An electrical conductor used to establish a contact with a nonmetalic part of a circuit such as a semiconductor, an electrolyte, etc.

Electrolyte: Substances that dissolve in polar solvents such as water, to produce an electrically conducting solution.

Entropy: A measure of the degree of randomness or disorderliness in a system. A "negative entropy" (negentropy) refers to increasing orderliness in a system.

Equivalent circuits: Theoretical circuits that retains all the electrical properties of a given circuit.

Grounding impedance: The resistance offered by the ground electrode to the flow of AC current into the ground. This is the ratio of the potential of the ground electrode to the current injected by it (i.e., I_g = potential to ground/current = V/I).

Impedance spectrum and spectroscopy: Impedance spectrum is a plot of impedance v_s frequency, which reveals the change of impedance of a sample with frequency during excitation by alternating current. Spectroscopy is the process of using impedance spectrum to analyze the dielectric property of a material as a function of frequency.

Inversion and tomography: Tomography is the process of recording a projection series from different angles and then using computational reconstruction to produce the image of the object in three dimensions (tomograms).

Ion pumps and ion channels: These are assemblies of integral membrane proteins that regulate the transport of ions into and out of cells or organelles, resulting in the generation of electrical signals. "Ion pumps" actively transport ions against a concentration gradient, whereas "ion channels" allow a passive flow of ions down a concentration gradient.

Nonpolarizable electrodes: An electrode whose potential is not affected by the current passing through it. They are used to eliminate the electrode polarization effect that occurs when metals (e.g., stainless steel electrodes) are used.

Organelles: Tiny cellular structures that perform specific functions within a cell, examples include vacuole, nucleus, etc.

R-C circuit: An electric circuit composed of resistors and capacitors driven by a voltage or current source.

Relaxation time: The time required for a perturbed system to return back to equilibrium.

Resistor: A passive electrical component used to create resistance to the flow of current.

Senescence: The process of aging characterized by gradual deterioration of functional characteristics.

Suberization: This is the impregnation of cell walls with suberins resulting in the formation of cork tissues. These suberins are complex macromolecules (biopolymers) that form protective barriers to prevent water and nutrients from entering into the stele through the apoplast. In roots, suberins are formed in the cell walls of the endodermal cells, collectively known as the "Casparian strip."

Vacuole: These are membrane-bound sacs within the cytoplasm of a cell. They are very important in providing support and also help to perform other functions such as storage, waste disposal, and protection.

CONFLICT OF INTEREST

The authors declare no conflict of interest

ACKNOWLEDGMENTS

This research was funded by the Belgian National Fund for Scientific Research FNRS (FRS-FNRS). A.K. and J.A.H. acknowledge funding by the German Research Foundation under Germany's Excellence Strategy, EXC 2070-390732324-PhenoRob.

ORCID

Solomon Ehosioke https://orcid.org/0000-0002-9526-5532
Sathyanarayan Rao https://orcid.org/0000-0002-0071-5167
Sarah Garré https://orcid.org/0000-0001-9025-5282

REFERENCES

Abdel Aal, G. Z., Atekwana, E. A., & Atekwana, E. A. (2010). Effect of bioclogging in porous media on complex conductivity signatures. *Journal of Geophysical Research*, *115*(G3). https://doi.org/10.1029/2009jg001159

Abdel Aal, G. Z., Atekwana, E. A., Slater, L. D., & Atekwana, E. A. (2004). Effects of microbial processes on electrolytic and interfacial electrical properties of unconsolidated sediments. *Geophysical Research Letters*, *31*(12). https://doi.org/10.1029/2004GL020030

Abdel Aal, G. Z., Slater, L. D., & Atekwana, E. A. (2006). Induced-polarization measurements on unconsolidated sediments from a site of active hydrocarbon biodegradation. *Geophysics*, *71*(2). https://doi.org/10.1190/1.2187760

Ackmann, J. J. (1993). Complex bioelectric impedance measurement system for the frequency range from 5 Hz to 1 MHz. *Annals of Biomedical Engineering*, *21*, 135–146. https://doi.org/10.1007/BF02367609

Allred, B. J., Daniels, J. J., & Ehsani, M. R. (2008). *Agricultural geophysics*. Boca Raton, FL: CRC Press.

Amato, M., Basso, B., Cellano, G., Bitella, G., Morelli, G., & Rossi, R. (2008). In situ detection of tree root distribution and biomass by multielectrode resistivity imaging. *Tree Physiology*, *28*, 1441–1448. https://doi.org/10.1093/treephys/28.10.1441

Amato, M., Bitella, G., Rossi, R., Gomez, J. A., Lovelli, S., & Ferreira, G. (2009). Multi-electrode 3D resistivity imaging of alfalfa root zone. *European Journal of Agronomy*, *31*, 213–222. https://doi.org/10.1016/j.eja.2009.08.005

Amundson, R., Richter, D. D., Humphreys, G. S., Jobbágy, E. G., & Gaillardet, J. (2007). Coupling between biota and earth materials in the critical zone. *Elements*, *3*, 327–332.

Anderson, W. P., & Higinbotham, N. (1976). Electrical resistance of corn root segments. *Plant Physiology*, *57*, 137–141. https://doi.org/10.1104/pp.57.2.137

Andrenelli, M. C., Magini, S., Pellegrini, S., Perria, R., Vignozzi, N., & Costantini, E. A. C. (2013). The use of the ARP© system to reduce the costs of soil survey for precision viticulture. *Journal of Applied Geophysics*, *99*, 24–34. https://doi.org/10.1016/j.jappgeo.2013.09.012

Atekwana, E., & Slater, L. (2009). Biogeophysics: A new frontier in earth science research. *Reviews of Geophysics*, *47*(4). https://doi.org/10.1029/2009RG000285

Atekwana, E. A., Werkema, D. D., & Atekwana, E. A. (2006). Biogeophysics: The effects of microbial processes on geophysical properties of the shallow subsurface. In H. Vereecken, A. Binley, G. Cassiani, A. Revil, & K. Titov (Eds.), *Applied hydrogeophysics* (pp. 161–193).

Dordrecht, the Netherlands: Springer. https://doi.org/10.1007/978-1-4020-4912-5_6

Aubrecht, L., Stanek, Z., & Koller, J. (2006). Electrical measurement of the absorption surfaces of tree roots by the earth impedance method: 1. Theory. *Tree Physiology*, *26*, 1105–1112. https://doi.org/10.1093/treephys/26.9.1105

Aulen, M., & Shipley, B. (2012). Non-destructive estimation of root mass using electrical capacitance on ten herbaceous species. *Plant and Soil*, *355*, 41–49. https://doi.org/10.1007/s11104-011-1077-3

Beff, L., Günther, T., Vandoorne, B., Couvreur, V., & Javaux, M. (2013). Three-dimensional monitoring of soil water content in a maize field using electrical resistivity tomography. *Hydrology and Earth System Sciences*, *17*, 595–609. https://doi.org/10.5194/hess-17-595-2013

Bengough, A. G., Valentine, T. A., Mckenzie, B. M., Hallett, P. D., Dietrich, R., White, P. J., & Jones, H. G. (2009). Physical limitations to root growth : Screening, scaling and reality. In *International Symposium "Root Research and Application" RootRAP* (pp. 2–4). Vienna: Boku.

Bera, T. K., Bera, S., Kar, K., & Mondal, S. (2016). Studying the variations of complex electrical bio-impedance of plant tissues during boiling. *Procedia Technology*, *23*, 248–255. https://doi.org/10.1016/J.PROTCY.2016.03.024

Bera, T. K., Nagaraju, J., & Lubineau, G. (2016). Electrical impedance spectroscopy (EIS)-based evaluation of biological tissue phantoms to study multifrequency electrical impedance tomography (Mf-EIT) systems. *Journal of Visualization*, *19*, 691–713. https://doi.org/10.1007/s12650-016-0351-0

Besson, A., Cousin, I., Samouëlian, A., Boizard, H., & Richard, G. (2004). Structural heterogeneity of the soil tilled layer as characterized by 2D electrical resistivity surveying. *Soil Tillage Research*, *79*, 239–249. https://doi.org/10.1016/j.still.2004.07.012

Binley, A., Kruschwitz, S., Lesmes, D., & Kettridge, N. (2010). Exploiting the temperature effects on low frequency electrical spectra of sandstone: A comparison of effective diffusion path lengths. *Geophysics*, *75*(6). https://doi.org/10.1190/1.3483815

Breede, K., Kemna, A., Esser, O., Zimmermann, E., Vereecken, H., & Huisman, J. A. 2012. Spectral induced polarization measurements on variably saturated sand-clay mixtures. *Near Surface Geophysics*, *10*, 479–489. https://doi.org/10.3997/1873-0604.2012048

Brogi, C., Huisman, J. A., Pätzold, S., von Hebel, C., Weihermüller, L., Kaufmann, M. S., … Vereecken, H. (2019). Large-scale soil mapping using multi-configuration EMI and supervised image classification. *Geoderma*, *335*, 133–148. https://doi.org/10.1016/j.geoderma.2018.08.001

Burr, K. E., Hawkins, C. D. B., Hirondelle, L, S. J., Binder, W. D., George, M. F., & Repo, T. (2001). Methods for measuring cold hardiness of conifers. In F. J. Bigras & S. J. Colombo (Eds.), *Conifer cold hardiness* (pp. 369–401). Dordrecht, the Netherlands: Springer. https://doi.org/10.1007/978-94-015-9650-3_14

Cao, Y., Repo, T., Silvennoinen, R., Lehto, T., & Pelkonen, P. (2010). An appraisal of the electrical resistance method for assessing root surface area. *Journal of Experimental Botany*, *61*, 2491–2497. https://doi.org/10.1093/jxb/erq078

Cao, Y., Repo, T., Silvennoinen, R., Lehto, T., & Pelkonen, P. (2011). Analysis of willow root system by electrical impedance spectroscopy. *Journal of Experimental Botany*, *62*, 351–358. https://doi.org/10.1093/jxb/erq276

Carlson, C. H., & Smart, L. B. (2016). Electrical capacitance as a predictor of root dry weight in shrub willow (*Salix*; Salicaceae) parents and progeny. *Applications in Plant Sciences*, *4*(8). https://doi.org/10.3732/apps.1600031

Cassiani, G., Boaga, J., Vanella, D., Perri, M. T., & Consoli, S. (2015). Monitoring and modelling of soil–plant interactions: The joint use of ERT, sap flow and eddy covariance data to characterize the volume of an orange tree root zone. *Hydrology and Earth System Sciences*, *19*, 2213–2225. https://doi.org/10.5194/hess-19-2213-2015

Čermák, J., Cudlín, P., Gebauer, R., Børja, I., Martinková, M., Staněk, Z., … Nadezhdina, N. (2013). Estimating the absorptive root area in Norway spruce by using the common direct and indirect earth impedance methods. *Plant and Soil*, *372*, 401–415. https://doi.org/10.1007/s11104-013-1740-y

Cermak, J., Ulrich, R., Stanek, Z., Koller, J., & Aubrecht, L. (2006). Electrical measurement of tree root absorbing surfaces by the earth impedance method. 2. Verification based on allometric relationships and root severing experiments. *Tree Physiology*, *26*, 1113–1121. https://doi.org/10.1093/treephys/26.9.1113

Chloupek, O. (1972). The relationship between electric capacitance and some other parameters of plant roots. *Biologia Plantarum*, *14*, 227–230. https://doi.org/10.1007/BF02921255

Chloupek, O. (1977). Evaluation of the size of a plant's root system using its electrical capacitance. *Plant and Soil*, *48*, 525–532. https://doi.org/10.1007/BF02187258

Chloupek, O., Dostál, V., Středa, T., Psota, V., & Dvořáčková, O. (2010). Drought tolerance of barley varieties in relation to their root system size. *Plant Breeding*, *129*, 630–636. https://doi.org/10.1111/j.1439-0523.2010.01801.x

Cole, K. S. (1940). Permeability and impermeability of cell membranes for ions. *Cold Spring Harbor Symposia on Quantitative Biology*, *8*, 110–122. https://doi.org/10.1101/SQB.1940.008.01.013

Corona-Lopez, D. D. J., Sommer, S., Rolfe, S. A., Podd, F., & Rieve, B. D. (2019). Electrical impedance tomography as a tool for phenotyping plant roots. *Plant Methods*, *15*(1). https://doi.org/10.1186/s13007-019-0438-4

Corwin, D. L., & Lesch, S. M. (2003). Application of soil electrical conductivity to precision agriculture. *Agronomy Journal*, *95*, 455–471. https://doi.org/10.2134/agronj2003.0455

Coster, H. G. L., Chilcott, T. C., & Coster, A. C. F. (1996). Impedance spectroscopy of interfaces, membranes and ultrastructures. *Bioelectrochemistry and Bioenergetics*, *40*, 79–98. https://doi.org/10.1016/0302-4598(96)05064-7

Couvreur, V., Faget, M., Lobet, G., Javaux, M., Chaumont, F., & Draye, X. (2018). Going with the flow: Multiscale insights into the composite nature of water transport in roots. *Plant Physiology*, *178*, 1689–1703. https://doi.org/10.1104/pp.18.01006

Cseresnyés, I., Kabos, S., Takács, T., Vég, K. R., Vozáry, E., & Rajkai, K. (2017). An improved formula for evaluating electrical capacitance using the dissipation factor. *Plant and Soil*, *419*, 237–256. https://doi.org/10.1007/s11104-017-3336-4

Cseresnyés, I., Rajkai, K., & Takács, T. (2016). Indirect monitoring of root activity in soybean cultivars under contrasting moisture regimes by measuring electrical capacitance. *Acta Physiologiae Plantarum*, *38*(5). https://doi.org/10.1007/s11738-016-2149-z

Cseresnyés, I., Rajkai, K., & Vozáry, E. (2013). Role of phase angle measurement in electrical impedance spectroscopy. *International Agrophysics*, *27*, 377–383. https://doi.org/10.2478/intag-2013-0007

Cseresnyés, I., Szitár, K., Rajkai, K., Füzy, A., Mikó, P., Kovács, R., & Takács, T. (2018). Application of electrical capacitance method for prediction of plant root mass and activity in field-grown crops.

Frontiers in Plant Science, *9*. https://doi.org/10.3389/fpls.2018.00093

Cseresnyés, I., Takács, T., Füzy, A., & Rajkai, K. (2014). Simultaneous monitoring of electrical capacitance and water uptake activity of plant root system. *International Agrophysics*, *28*, 537–541. https://doi.org/10.2478/intag-2014-0044

Cseresnyés, I., Takács, T., Füzy, A., Végh, K. R., & Lehoczky, É. (2016). Application of electrical capacitance measurement for in situ monitoring of competitive interactions between maize and weed plants. *Spanish Journal of Agricultural Research*, *14*(2). https://doi.org/10.5424/sjar/2016142-7562

Cseresnyés, I., Takács, T., Végh, K. R., Anton, A., & Rajkai, K. (2013). Electrical impedance and capacitance method: A new approach for detection of functional aspects of arbuscular mycorrhizal colonization in maize. *European Journal of Soil Biology*, *54*, 25–31. https://doi.org/10.1016/J.EJSOBI.2012.11.001

Dalton, F. N. (1995). In-situ root extent measurements by electrical capacitance methods. *Plant and Soil*, *173*, 157–165. https://doi.org/10.1007/BF00155527

Deiana, R., Cassiani, G., Kemna, A., Villa, A., Bruno, V., & Bagliani, A. (2007). An experiment of non-invasive characterization of the vadose zone via water injection and cross-hole time-lapse geophysical monitoring. *Near Surface Geophysics*, *5*, 183–194. https://doi.org/10.3997/1873-0604.2006030

De-la-Peña, C., & Loyola-Vargas, V. M. (2014). Biotic interactions in the rhizosphere: A diverse cooperative enterprise for plant productivity. *Plant Physiology*, *166*, 701–719. https://doi.org/10.1104/pp.114.241810

Dick, J., Tetzlaff, D., Bradford, J., & Soulsby, C. (2018). Using repeat electrical resistivity surveys to assess heterogeneity in soil moisture dynamics under contrasting vegetation types. *Journal of Hydrology*, *559*, 684–697. https://doi.org/10.1016/J.JHYDROL.2018.02.062

Dietrich, R. C., Bengough, A. G., Jones, H. G., & White, P. J. (2012). A new physical interpretation of plant root capacitance. *Journal of Experimental Botany*, *63*, 6149–6159. https://doi.org/10.1093/jxb/ers264

Dietrich, R. C., Bengough, A. G., Jones, H. G., & White, P. J. (2013). Can root electrical capacitance be used to predict root mass in soil? *Annals of Botany*, *112*, 457–464. https://doi.org/10.1093/aob/mct044

Doolittle, J. A., Sudduth, K. A., Kitchen, N. R., & Indorante, S. J. (1994). Estimating depths to claypans using electromagnetic induction methods. *Journal of Soil and Water Conservation*, *49*, 572–575.

Ehosioke, S., Garre, S., Kremer, T., Rao, S., Kemna, A., Huisman, J. A., … Nguyen, F. (2018). A new method for characterizing the complex electrical properties of root segments. Paper presented at the 10th Symposium of the International Society of Root Research, Ma'ale Hahamisha, Israel.

Ehosioke, S., Phalempin, M., Garre, S., Kemna, A., Huisman, J. A., Javaux, M., & Nguyen, F. (2017). Developing suitable methods for effective characterization of electrical properties of root segments. In Geophysical research abstracts (Vol. 19). Vienna: European Geosciences Union. Retrieved from http://hdl.handle.net/2268/213406

Ellis, T., Murray, W., & Kavalieris, L. (2013). Electrical capacitance of bean (*Vicia faba*) root systems was related to tissue density: A test for the Dalton model. *Plant and Soil*, *366*, 575–584 https://doi.org/10.1007/s11104-012-1424-z

Ellis, T. W., Murray, W., Paul, K., Kavalieris, L., Brophy, J., Williams, C., & Maass, M. (2013). Electrical capacitance as a rapid and non-invasive indicator of root length. *Tree Physiology*, *33*, 3–17. https://doi.org/10.1093/treephys/tps115

Freeland, R. S., Yoder, R. E., & Ammons, J. T. (1998). Mapping shallow underground features that influence site-specific agricultural production. *Journal of Applied Geophysics*, *40*, 19–27. https://doi.org/10.1016/S0926-9851(98)00014-7

Frensch, J., & Steudle, E. (1989). Axial and radial hydraulic resistance to roots of maize (*Zea mays* L.). *Plant Physiology*, *91*, 719–726. https://doi.org/10.1104/pp.91.2.719

Garré, S., Coteur, I., Wongleecharoen, C., Kongkaew, T., Diels, J., & Vanderborght, J. (2013). Noninvasive monitoring of soil water dynamics in mixed cropping systems: A case study in Ratchaburi Province, Thailand. *Vadose Zone Journal*, *12*(2). https://doi.org/10.2136/vzj2012.0129

Garré, S., Günther, T., Diels, J., & Vanderborght, J. (2012). Evaluating experimental design of ERT for soil moisture monitoring in contour hedgerow intercropping systems. *Vadose Zone J*, *11*(4). https://doi.org/10.2136/vzj2011.0186

Garré, S., Javaux, M., Vanderborght, J., Pages, L., & Vereecken, H. (2011). Three-dimensional electrical resistivity tomography to monitor root zone water dynamics. *Vadose Zone J*, *10*, 412–424. https://doi.org/10.2136/vzj2010.0079

Hagrey, S. A. (2007). Geophysical imaging of root-zone, trunk, and moisture. *Journal of Experimental Botany*, *58*, 839–854. https://doi.org/10.1093/jxb/erl237

Hagrey, S. A., & Michaelsen, J. (2002). Hydrogeophysical soil study at a drip irrigated orchard, Portugal. *European Journal of Environmental and Engineering Geophysics*, *7*, 75–93.

Hanafy, S., & Hagrey, S. A. (2006). Ground-penetrating radar tomography for soil-moisture heterogeneity. *Geophysics*, *71*, k9–k18. https://doi.org/10.1190/1.2159052

Hayden, R. I., Moyse, C. A., Calder, F. W., Crawford, D. P., & Fensom, D. S. (1969). Electrical impedance studies on potato and alfalfa tissue. *Journal of Experimental Botany*, *20*, 177–200. https://doi.org/10.1093/jxb/20.2.177

Hille, B. (2001). *Ion channels of excitable membranes* (3rd ed.). Sunderland, MA: Sinauer Associates.

Huisman, J. A., Snepvangers, J. J. J. C., Bouten, W., & Heuvelink, G. B. M. (2002). Mapping spatial variation in surface soil water content: Comparison of ground-penetrating radar and time domain reflectometry. *Journal of Hydrology*, *269*, 194–207. https://doi.org/10.1016/S0022-1694(02)00239-1

Inaba, A., Manabe, T., Tsuji, H., & Lwamoto, T. (1995). Electrical lmpedance analysis of tissue properties associated with ethylene induction by electric currents in cucumber (*Cucumis sativus* L.) fruit. *Plant Physiology*, *107*, 199–205. https://doi.org/10.1104/pp.107.1.199

Jayawickreme, D. H., Jobbágy, E. G., & Jackson, R. B. (2014). Geophysical subsurface imaging for ecological applications. *New Phytologist*, *201*, 1170–1175. https://doi.org/10.1111/nph.12619

Jayawickreme, D. H., Van Dam, R. L., & Hyndman, D. W. (2008). Subsurface imaging of vegetation, climate, and root-zone moisture interactions. *Geophysical Research Letters*, *35*(18). https://doi.org/10.1029/2008GL034690

Jayawickreme, D. H., Van Dam, R. L., & Hyndman, D. W. (2010). Hydrological consequences of land-cover change: Quantifying the influence of plants on soil moisture with time-lapse electrical resistivity. *Geophysics*, *75*, WA43–WA50. https://doi.org/10.1190/1.3464760

Jaynes, D. B., Novak, J. M., Moorman, T. B., & Cambardella, C. A. (1995). Estimating herbicide partition coefficients from electromagnetic induction measurements. *Journal of Environment Quality*, *24*, 36–41. https://doi.org/10.2134/jeq1995.00472425002400010005x

Jocsac, I., Vegvari, G., & Vozary, E. (2019). Electrical impedance measurement on plants: A review with some insights to other fields. *Theoretical and Experimental Plant Physiology*, *31*, 359–375. https://doi.org/10.1007/s40626-019-00152-y

Jonard, F., Mahmoudzadeh, M., Roisin, C., Weihermüller, L., André, F., Minet, J., … Lambot, S. (2013). Characterization of tillage effects on the spatial variation of soil properties using ground-penetrating radar and electromagnetic induction. *Geoderma*, *207–208*, 310–322. https://doi.org/10.1016/j.geoderma.2013.05.024

Jougnot, D., Ghorbani, A., Revil, A., Leroy, P., & Cosenza, P. (2010). Spectral induced polarization of partially saturated clay-rocks: A mechanistic approach. *Geophysical Journal International*, *180*, 210–224. https://doi.org/10.1111/j.1365-246X.2009.04426.x

Kachanoski, R. G., Wesenbeeck, I. J. Van, & Gregorich, E. G. (1988). Estimating spatial variations of soil water content using noncontacting electromagnetic inductive methods. *Canadian Journal of Soil Science*, *68*, 715–722. https://doi.org/10.4141/cjss88-069

Kao, K. C. (2004). *Dielectric phenomena in solids with emphasis on physical concepts of electronic processes*. San Diego, CA: Elsevier Academic Press.

Katul, G., Todd, P., Pataki, D., Kabala, Z. J., & Oren, R. (1997). Soil water depletion by oak trees and the influence of root water uptake on the moisture content spatial statistics. *Water Resources Research*, *33*, 611–623. https://doi.org/10.1029/96WR03978

Kemna, A., Binley, A., Cassiani, G., Niederleithinger, E., Revil, A., Slater, L., … Zimmermann, E. (2012). An overview of the spectral induced polarization method for near-surface applications. *Near Surface Geophysics*, *10*, 453–468. https://doi.org/10.3997/1873-0604.2012027

Kendall, W. A., Pederson, G. A., & Hill, R. R. (1982). Root size estimates of red clover and alfalfa based on electrical capacitance and root diameter measurements. *Grass and Forage Science*, *37*, 253–256. https://doi.org/10.1111/j.1365-2494.1982.tb01604.x

Kessouri, P., Furman, A., Huisman, J. A., Martin, T., Mellage, A., Ntarlagiannis, D., … Placencia-Gomez, E. (2019). Induced polarization applied to biogeophysics: Recent advances and future prospects. *Near Surface Geophysics*, *17*, 595–621. https://doi.org/10.1002/nsg.12072

Kinraide, T. B. (2001). Ion fluxes considered in terms of membrane surface electrical potentials. *Australian Journal of Plant Physiology*, *28*, 607–618.

Kinraide, T. B., & Wang, P. (2010). The surface charge density of plant cell membranes (σ): An attempt to resolve conflicting values for intrinsic σ. *Journal of Experimental Botany*, *61*, 2507–2518. https://doi.org/10.1093/jxb/erq082

Kitchen, N. R., Sudduth, K. A., & Drummond, S. T. (1999). Soil electrical conductivity as a crop productivity measure for claypan soils. *Journal of Production Agriculture*, *12*, 607–617. https://doi.org/10.2134/jpa1999.0607

Klauke, S., Fischer, H., Rieger, A., Frühauf, L., Staszewski, S., Althoff, P.-H., & Helm, E. B. (2005). Use of bioelectrical impedance analysis to determine body composition changes in HIV-associated wasting. *International Journal of STD & AIDS*, *16*, 307–313. https://doi.org/10.1258/0956462053654177

Konstantinovic, M., Wöckel, S., Schulze Lammers, P., Sachs, J., & Martinov, M. (2007). Detection of root biomass using ultra-wideband radar: An approach to potato nest positioning. *International Commission of Agricultural Engineering*. Retrieved from http://hdl.handle.net/1813/10662

Kormanek, M., Głąb, T., & Klimek-Kopyra, A. (2016). Modification of the tree root electrical capacitance method under laboratory conditions. *Tree Physiology*, *36*, 121–127. https://doi.org/10.1093/treephys/tpv088

Koumanov, K. S., Hopmans, J. W., & Schwankl, L. W. (2006). Spatial and temporal distribution of root water uptake of an almond tree under microsprinkler irrigation. *Irrigation Science*, *24*, 267–278. https://doi.org/10.1007/s00271-005-0027-3

Lazzari, L., Celano, G., Amato, M., Hagrey, Al, A., S., Loperte, A., … Lapenna, V. (2008). Spatial variability of soil root zone properties using electrical imaging techniques in a peach orchard system. *Geophysical Research Abstracts*, *10*, 712.

Lin, C.-M., Chen, L.-H., & Chen, T. M. (2012). The development and application of an electrical impedance spectroscopy measurement system for plant tissues. *Computers and Electronics in Agriculture*, *82*, 96–99. https://doi.org/10.1016/J.COMPAG.2011.10.017

Longui, E. L., Romeiro, D., & Alves, E. S. (2012). Differences in anatomy and potential hydraulic conductivity between root and stem of *Caesalpinia echinata* Lam. (Fabaceae). *Hoehnea*, *39*, 649–655. https://doi.org/10.1590/s2236-89062012000400010

Looms, M. C., Jensen, K. H., Binley, A., & Nielsen, L. (2008). Monitoring unsaturated flow and transport using cross-borehole geophysical methods. *Vadose Zone Journal*, *7*, 227–237. https://doi.org/10.2136/vzj2006.0129

Loperte, A., Satriani, A., Lazzari, L., Amato, M., Celano, G., Lapenna, V., & Morelli, G. (2006). 2D and 3D high resolution geoelectrical tomography for non-destructive determination of the spatial variability of plant root distribution: Laboratory experiments and field measurements. *Geophysical Research Abstracts*, *8*, 06749.

Lu, Z., Hickey, C. J., & Sabatier, J. M. (2004). Effects of compaction on the acoustic velocity in soils. *Soil Science Society of America Journal*, *68*, 7–16. https://doi.org/10.2136/sssaj2004.7000

Lu, Z., & Sabatier, J. M. (2009). Effects of soil water potential and moisture content on sound speed. *Soil Science Society of America Journal*, *73*, 1614–1625. https://doi.org/10.2136/sssaj2008.0073

Macdonald, J. R. (1987). *Impedance spectroscopy: Emphasizing solid materials and systems*. New York: Wiley.

Macdonald, J. R. (1992). Impedance spectroscopy. *Annals of Biomedical Engineering*, *20*, 289–305. https://doi.org/10.1007/BF02368532

Maeght, J. L., Rewald, B., & Pierret, A. (2013). How to study deep roots-and why it matters. *Frontiers in Plant Science*, *4*. https://doi.org/10.3389/fpls.2013.00299

Mares, R., Barnard, H. R., Mao, D., Revil, A., & Singha, K. (2016). Examining diel patterns of soil and xylem moisture using electrical resistivity imaging. *Journal of Hydrology*, *536*, 327–338. https://doi.org/10.1016/j.jhydrol.2016.03.003

Martin, T., Nordsiek, S., & Weller, A. (2015). Low-frequency impedance spectroscopy of wood. *Journal of Research in Spectroscopy*, *2015*. https://doi.org/10.5171/2015.910447

Martinez, F. J., Batzle, M. L., & Revil, A. (2012). Influence of temperature on seismic velocities and complex conductivity of heavy oil-bearing sands. *Geophysics*, *77*(3). https://doi.org/10.1190/geo2011-0433.1

Mary, B., Abdulsamad, F., Saracco, G., Peyras, L., Vennetier, M., Mériaux, P., & Camerlynck, C. (2017). Improvement of coarse root detec-

tion using time and frequency induced polarization: From laboratory to field experiments. *Plant and Soil*, *417*, 243–259. https://doi.org/10.1007/s11104-017-3255-4

Mary, B., Peruzzo, L., Boaga, J., Schmutz, M., Wu, Y., Hubbard, S. S., & Cassiani, G. (2018). Small-scale characterization of vine plant root water uptake via 3-D electrical resistivity tomography and mise-à-la-masse method. *Hydrology and Earth System Sciences*, *22*, 5427–5444. https://doi.org/10.5194/hess-22-5427-2018

Mary, B., Saracco, G., Peyras, L., Vennetier, M., Mériaux, P., & Camerlynck, C. (2016). Mapping tree root system in dikes using induced polarization: Focus on the influence of soil water content. *Journal of Applied Geophysics*, *135*, 387–396. https://doi.org/10.1016/j.jappgeo.2016.05.005

Mary, B., Vanella, D., Consoli, S., & Cassiani, G. (2019). Assessing the extent of citrus trees root apparatus under deficit irrigation via multi-method geo-electrical imaging. *Scientific Reports*, *9*(1). https://doi.org/10.1038/s41598-019-46107-w

Mathie, A., Kennard, L. E., & Veale, E. L. (2003). Neuronal ion channels and their sensitivity to extremely low frequency weak electric field effects. *Radiation Protection Dosimetry*, *106*, 311–315. https://doi.org/10.1093/oxfordjournals.rpd.a006365

Mcbride, R., Candido, M., & Ferguson, J. (2008). Estimating root mass in maize genotypes using the electrical capacitance method. *Archives of Agronomy and Soil Science*, *54*, 215–226. https://doi.org/10.1080/03650340701790658

Michot, D., Benderitter, Y., Dorigny, A., Nicoullaud, B., King, D., & Tabbagh, A. (2003). Spatial and temporal monitoring of soil water content with an irrigated corn crop cover using surface electrical resistivity tomography. *Water Resources Research*, *39*(5). https://doi.org/10.1029/2002WR001581

Moreno, Z., Arnon-zur, A., & Furman, A. (2015). Hydro-geophysical monitoring of orchard root zone dynamics in semi-arid region. *Irrigation Science*, *33*, 303–318. https://doi.org/10.1007/s00271-015-0467-3

Nguyen, C. (2009). Rhizodeposition of organic C by plant: Mechanisms and controls. In E. Lichtfouse, M. Navarrete, D. Debaeke, S. Véronique, & C. Alberola (Eds.), *Sustainable agriculture* (pp. 97–123). Dordrecht, the Netherlands: Springer. https://doi.org/10.1007/978-90-481-2666-8_9

Ni, J.-J., Cheng, Y.-F., Bordoloi, S., Bora, H., Wang, Q.-H., Ng, C.-W.-W., & Garg, A. (2018). Investigating plant root effects on soil electrical conductivity: An integrated field monitoring and statistical modelling approach. *Earth Surface Processes and Landforms*, *44*, 825–839. https://doi.org/10.1002/esp.4533

Ntarlagiannis, D., Williams, K. H., Slater, L., & Hubbard, S. (2005). Low-frequency electrical response to microbial induced sulfide precipitation. *Journal of Geophysical Research: Biogeosciences*, *110*(G2). https://doi.org/10.1029/2005jg000024

Oberdörster, C., Vanderborght, J., Kemna, A., & Vereecken, H. (2010). Investigating preferential flow processes in a forest soil using time domain reflectometry and electrical resistivity tomography. *Vadose Zone Journal*, *9*, 350–361. https://doi.org/10.2136/vzj2009.0073

Ozier-Lafontaine, H., & Bajazet, T. (2005). Analysis of root growth by impedance spectroscopy (EIS). *Plant and Soil*, *277*, 299–313. https://doi.org/10.1007/s11104-005-7531-3

Paglis, C. M. (2013). Application of electrical resistivity tomography for detecting root biomass in coffee trees. *International Journal of Geophysics*, *2013*. https://doi.org/10.1155/2013/383261

Panissod, C., Michot, D., Benderitter, Y., & Tabbagh, A. (2001). On the effectiveness of 2D electrical inversion results: An agricultural case study. *Geophysical Prospecting*, *49*, 570–576. https://doi.org/10.1046/j.1365-2478.2001.00277.x

Parasnis, D. S. (1967). Three-dimensional electric mise-a-la-masse survey of an irregular lead-zinc-copper deposit in central Sweden. *Geophysical Prospecting*, *15*, 407–437. https://doi.org/10.1111/j.1365-2478.1967.tb01796.x

Peruzzo, L., Chou, C., Wu, Y., Schmutz, M., Mary, B., Wagner, F. M., … Hubbard, S. (2020). Imaging of plant current pathways for non-invasive root phenotyping using a newly developed electrical current source density approach. *Plant and Soil*, *450*, 567–584. https://doi.org/10.1007/s11104-020-04529-w

Peterson, T., & Al Hagrey, S. A. (2009). Mapping root zones of small plants using surface and borehole resistivity tomography. *The Leading Edge*, *7*, 1220–1224. https://doi.org/10.1190/1.3249778

Pitre, F. E., Brereton, N. J. B., Audoire, S., Richter, G. M., Shield, I., & Karp, A. (2010). Estimating root biomass in *Salix viminalis* × *Salix schwerinii* cultivar "Olof" using the electrical capacitance method. *Plant Biosystems*, *144*, 479–483. https://doi.org/10.1080/11263501003732092

Postic, F., & Doussan, C. (2016). Benchmarking electrical methods for rapid estimation of root biomass. *Plant Methods*, *12*(1). https://doi.org/10.1186/s13007-016-0133-7

Preston, G. M., McBride, R. A., Bryan, J., & Candido, M. (2004). Estimating root mass in young hybrid poplar trees using the electrical capacitance method. *Agroforestry Systems*, *60*, 305–309. https://doi.org/10.1023/B:AGFO.0000024439.41932.e2

Prodan, E., Prodan, C., & Miller, J. H. (2008). The dielectric response of spherical live cells in suspension: An analytic solution. *Biophysical Journal*, *95*, 4174–4182. https://doi.org/10.1529/BIOPHYSJ.108.137042

Rajkai, K., Végh, K. R., & Nacsa, T. (2005). Electrical capacitance of roots in relation to plant electrodes, measuring frequency and root media. *Acta Agronomica Hungarica*, *53*, 197–210. https://doi.org/10.1556/AAgr.53.2005.2.8

Rao, S., Lesparre, N., Orozco, A. F., Wagner, F., & Javaux, M. (2020). Imaging plant responses to water deficit using electrical resistivity tomography. *Plant and Soil*, *454*, 261–281. https://doi.org/10.1007/s11104-020-04653-7

Rao, S., Meunier, F., Ehosioke, S., Lesparre, N., Kemna, A., Nguyen, F., … Javaux, M. (2019). Impact of maize roots on soil–root electrical conductivity: A simulation study. *Vadose Zone Journal*, *18*(1). https://doi.org/10.2136/vzj2019.04.0037

Raven, P., Johnson, G., Mason, K., Losos, J., & Singer, S. (2017). *Biology* (11th ed.). New York: McGraw-Hill Education.

Repo, T., Cao, Y., Silvennoinen, R., & Ozier-Lafontaine, H. (2012). Electrical impedance spectroscopy and roots. In S. Mancuso (Ed.), *Measuring roots* (pp. 25–49). Berlin, Heidelberg: Springer. https://doi.org/10.1007/978-3-642-22067-8_2

Repo, T., Korhonen, A., Laukkanen, M., Lehto, T., & Silvennoinen, R. (2014). Detecting mycorrhizal colonisation in Scots pine roots using electrical impedance spectra. *Biosystems Engineering*, *121*, 139–149. https://doi.org/10.1016/j.biosystemseng.2014.02.014

Repo, T., Korhonen, A., Lehto, T., & Silvennoinen, R. (2016). Assessment of frost damage in mycorrhizal and non-mycorrhizal roots of Scots pine seedlings using classification analysis of their electrical impedance spectra. *Trees*, *30*, 483–495. https://doi.org/10.1007/s00468-015-1171-x

Repo, T., Laukkanen, J., & Silvennoinen, R. (2005). Measurement of the tree root growth using electrical impedance spectroscopy. *Silva Fennica*, *39*, 159–166. Retrieved from https://silvafennica.fi/pdf/article380.pdf

Repo, T., Zhang, G., Ryyppö, A., & Rikala, R. (2000). The electrical impedance spectroscopy of scots pine (*Pinus sylvestris* L.) shoots in relation to cold acclimation. *Journal of Experimental Botany*, *51*, 2095–2107. https://doi.org/10.1093/jexbot/51.353.2095

Repo, T., Zhang, M. I. N., Ryyppö, A., Vapaavuori, E., & Sutinen, S. (1994). Effects of freeze-thaw injury on parameters of distributed electrical circuits of stems and needles of Scots pine seedlings at different stages of acclimation. *Journal of Experimental Botany*, *45*, 823–833. https://doi.org/10.1093/jxb/45.6.823

Revil, A., & Florsch, N. (2010). Determination of permeability from spectral induced polarization in granular media. *Geophysical Journal International*, *181*, 1480–1498. https://doi.org/10.1111/j.1365-246X.2010.04573.x

Revil, A., Schmutz, M., & Batzle, M. L. (2011). Influence of oil wettability upon spectral induced polarization of oil-bearing sands. *Geophysics*, *76*(5). https://doi.org/10.1190/geo2011-0006.1

Ristic, A., Petrovacki, D., & Vrtunski, M. (2014). Ground penetrating radar technology: The usage in agriculture. *Research Journal of Agricultural Science*, *46*, 53–58.

Robert, P. C., Rust, R. H., Larson, W. E., Jaynes, D. B., Colvin, T. S., & Ambuel, J. (1995). Yield mapping by electromagnetic induction. In P. C. Robert, R. H. Rust, & W. E. Larson (Eds.), *Site-specific management for agricultural systems* (pp. 383–394). Madison, WI: ASA, CSSA, and SSSA. https://doi.org/10.2134/1995.site-specificmanagement.c26

Robinson, J. L., Slater, L. D., & Schäfer, K. V. R. (2012). Evidence for spatial variability in hydraulic redistribution within an oak-pine forest from resistivity imaging. *Journal of Hydrology*, *430–431*, 69–79. https://doi.org/10.1016/j.jhydrol.2012.02.002

Rodríguez-Robles, U., Arredondo, T., Huber-Sannwald, E., Ramos-Leal, J. A., & Yépez, E. A. (2017). Application of geophysical tools for tree root studies in forest ecosystems in complex soils. *Biogeosciences*, *14*, 5343–5357. https://doi.org/10.5194/bg-14-5343-2017

Rohatgi, A. (2011). WebPlotDigitizer, Ankit Rohatgi. Retrieved from https://automeris.io/WebPlotDigitizer/

Rossi, R., Amato, M., Bitella, G., Bochicchio, R., Ferreira Gomes, J. J., Lovelli, S., … Favale, P. (2011). Electrical resistivity tomography as a non-destructive method for mapping root biomass in an orchard. *European Journal of Soil Science*, *62*, 206–215. https://doi.org/10.1111/j.1365-2389.2010.01329.x

Rossi, R., Pollice, A., Diago, M.-P., Oliveira, M., Millan, B., Bitella, G., … Tardaguila, J. (2013). Using an automatic resistivity profiler soil sensor on-the-go in precision viticulture. *Sensors*, *13*, 1121–1136. https://doi.org/10.3390/s130101121

Schmutz, M., Revil, A., Vaudelet, P., Batzle, M., Viñao, P. F., & Werkema, D. D. (2010). Influence of oil saturation upon spectral induced polarization of oil-bearing sands. *Geophysical Journal International*, *183*, 211–224. https://doi.org/10.1111/j.1365-246X.2010.04751.x

Schwan, H. P. (1957). Electrical properties of tissue and cell suspensions. *Advances in Biological and Medical Physics*, *5*, 147–209. https://doi.org/10.1016/B978-1-4832-3111-2.50008-0

Schwan, H. P. (1963). Determination of biological impedances. In WL. Nastuk (Ed.), *Physical techniques in biological research* (Vol. 6, pp. 323–406). New York: Academic Press.

Schwan, H. P. (1988). Biological effects of non-ionizing radiations: Cellular properties and interactions. *Annals of Biomedical Engineering*, *16*, 245–263. https://doi.org/10.1007/BF02368002

Schwan, H. P., & Takashima, S. (1991). Dielectric behaviour of biological cells and membranes. *Bulletin of the Institute for Chemical Research*, *69*, 459–475.

Schwartz, N., & Furman, A. (2015). On the spectral induced polarization signature of soil organic matter. *Geophysical Journal International*, *200*, 589–595. https://doi.org/10.1093/gji/ggu410

Shrivastava, B. D., Barde, R., Mishra, A., & Phadke, S. (2014a). Dielectric behavior of biomaterials at different frequencies on room temperature. *Journal of Physics: Conference Series*, *534*. https://doi.org/10.1088/1742-6596/534/1/012063

Shrivastava, B. D., Barde, R., Mishra, A., & Phadke, S. (2014b). Interaction of electromagnetic fields and biological tissues. *Journal of Physics: Conference Series*, *534*. http://doi.org/10.1088/1742-6596/534/1/012062

Simard, S. W., Jones, M. D., & Durall, D. M. (2003). Carbon and nutrient fluxes within and between mycorrhizal plants. In M. G. A. van der Heijden & I. R. Sanders (Eds.), *Mycorrhizal ecology* (pp. 33–74). https://doi.org/10.1007/978-3-540-38364-2_2

Skold, M., Revil, A., & Vaudelet, P. (2011). The pH dependence of spectral induced polarization of silica sands: Experiment and modeling. *Geophysical Research Letters*, *38*(12). https://doi.org/10.1029/2011GL047748

Srayeddin, I., & Doussan, C. (2009). Estimation of the spatial variability of root water uptake of maize and sorghum at the field scale by electrical resistivity tomography. *Plant and Soil*, *319*, 185–207. https://doi.org/10.1007/s11104-008-9860-5

Srinivas, K., Sarah, P., & Suryanarayana, S. V. (2003). Impedance spectroscopy study of polycrystalline $Bi_6Fe_2Ti_3O_{18}$. *Bulletin of Materials Science*, *26*, 247–253. https://doi.org/10.1007/BF02707799

Sudduth, K. A., Drummond, S. T., & Kitchen, N. R. (2001). Accuracy issues in electromagnetic induction sensing of soil electrical conductivity for precision agriculture. *Computers and Electronics in Agriculture*, *31*, 239–264. https://doi.org/10.1016/S0168-1699(00)00185-X

Tresoldi, G., Arosio, D., Hojat, A., Longoni, L., Papini, M., & Zanzi, L. (2019). Long-term hydrogeophysical monitoring of the internal conditions of river levees. *Engineering Geology*, *259*. https://doi.org/10.1016/j.enggeo.2019.05.016

Tsukahara, K., Yamane, K., Yamaki, Y., & Honjo, H. (2009). A non-destructive method for estimating the root mass of young peach trees after root pruning using electrical capacitance measurements. *Journal of Agricultural Meteorology*, *65*, 209–213. https://doi.org/10.2480/agrmet.65.2.6

Tsukanov, K., & Schwartz, N. (2020). Relationship between wheat root properties and its electrical signature using the spectral induced polarization method. *Vadose Zone Journal*, *19*(1). https://doi.org/10.1002/vzj2.20014

Urban, J., Bequet, R., & Mainiero, R. (2011). Assessing the applicability of the earth impedance method for in situ studies of tree root systems. *Journal of Experimental Botany*, *62*, 1857–1869. https://doi.org/10.1093/jxb/erq370

van Beem, J., Smith, M. E., & Zobel, R. W. (1998). Estimating root mass in maize using a portable capacitance meter. *Agronomy Journal*, *90*, 566–570. https://doi.org/10.2134/agronj1998.00021962009000040021x

van Treeck, S., Zimmermann, E., Weigand, M., Huisman, J. A., & Kemna, A. (2017). *Developing an electrode design for EIT field measurements on crop root systems*. Paper presented at the 4th International workshop on geoelectrical monitoring, Vienna. https://doi.org/10.13140/RG.2.2.31080.32009

Vanderborght, J., Huisman, J. A., Kruk, J. van der, Vereecken, H., Anderson, S. H., & Hopmans, J. W. (2013). Geophysical methods for field-scale imaging of root zone properties and processes. In S. H. Anderson & J. W. Hopmans (Eds.), *Soil–water–root processes: advances in tomography and imaging* (Vol. 61, pp. 247–282). Madison, WI: SSSA. https://doi.org/10.2136/sssaspecpub61.c12

Vanella, D., Cassiani, G., Busato, L., Boaga, J., Barbagallo, S., Binley, A., & Consoli, S. (2018). Use of small scale electrical resistivity tomography to identify soil-root interactions during deficit irrigation. *Journal of Hydrology*, *556*, 310–324. https://doi.org/10.1016/J.JHYDROL.2017.11.025

Vaudelet, P., Revil, A., Schmutz, M., Franceschi, M., & Bégassat, P. (2011). Changes in induced polarization associated with the sorption of sodium, lead, and zinc on silica sands. *Journal of Colloid and Interface Science*, *360*, 739–752. https://doi.org/10.1016/j.jcis.2011.04.077

Vereecken, H., Binley, A., Cassiani, G., Revil, A., & Titov, K. (2007). Applied hydrogeophysics. In H. Vereecken, A. Binley, G. Cassiani, A. Revil, & K. Titov (Eds.), *Applied hydrogeophysics* (pp. 1–8). Dordrecht, the Netherlands: Springer. https://doi.org/10.1007/978-1-4020-4912-5_1

von Hebel, C., Matveeva, M., Verweij, E., Rademske, P., Kaufmann, M. S., Brogi, C., … van der Kruk, J. (2018). Understanding soil and plant interaction by combining ground-based quantitative electromagnetic induction and airborne hyperspectral data. *Geophysical Research Letters*, *45*, 7571–7579. https://doi.org/10.1029/2018GL078658

Wang, P., Kinraide, T. B., Zhou, D., Kopittke, P. M., & Peijnenburg, W. J. G.M. (2011). Plasma membrane surface potential: Dual effects upon ion uptake and toxicity. *Plant Physiology*, *155*, 808–820. https://doi.org/10.1104/pp.110.165985

Weigand, M. (2017). *Monitoring structural and physiological properties of crop roots using spectral electrical impedance tomography* (Doctoral dissertation, Univerity of Bonn). https://doi.org/10.5281/zenodo.400833

Weigand, M., & Kemna, A. (2016). Debye decomposition of time-lapse spectral induced polarisation data. *Computers and Geosciences*, *86*, 34–45. https://doi.org/10.1016/j.cageo.2015.09.021

Weigand, M., & Kemna, A. (2017). Multi-frequency electrical impedance tomography as a non-invasive tool to characterize and monitor crop root systems. *Biogeosciences*, *14*, 921–939. https://doi.org/10.5194/bg-14-921-2017

Weigand, M., & Kemna, A. (2019). Imaging and functional characterization of crop root systems using spectroscopic electrical impedance measurements. *Plant and Soil*, *435*, 201–224. https://doi.org/10.1007/s11104-018-3867-3

Weihermüller, L., Huisman, J. A., Lambot, S., Herbst, M., & Vereecken, H. (2007). Mapping the spatial variation of soil water content at the field scale with different ground penetrating radar techniques. *Journal of Hydrology*, *340*, 205–216. https://doi.org/10.1016/j.jhydrol.2007.04.013

Weller, A., Breede, K., Slater, L., & Nordsiek, S. (2011). Effect of changing water salinity on complex conductivity spectra of sandstones. *Geophysics*, *76*(5). https://doi.org/10.1190/geo2011-0072.1

Werban, U., Attia al Hagrey, S., & Rabbel, W. (2008). Monitoring of root-zone water content in the laboratory by 2D geoelectrical tomography. *Journal of Plant Nutrition and Soil Science*, *171*, 927–935. https://doi.org/10.1002/jpln.200700145

Williams, B., Walker, J., & Anderson, J. (2006). Spatial variability of regolith leaching and salinity in relation to Whole Farm Planning. *Australian Journal of Experimental Agriculture*, *46*, 1271–1277. https://doi.org/10.1071/EA04110

Yoder, R. E., Freeland, R. S., Ammons, J. T., & Leonard, L. L. (2001). Mapping agricultural fields with GPR and EMI to identify offsite movement of agrochemicals. *Journal of Applied Geophysics*, *47*, 251–259. https://doi.org/10.1016/S0926-9851(01)00069-6

Zenone, T., Morelli, G., Teobaldelli, M., Fischanger, F., Matteucci, M., Sordini, M., … Seufert, G. (2008). Preliminary use of ground-penetrating radar and electrical resistivity tomography to study tree roots in pine forests and poplar plantations. *Functional Plant Biology*, *35*, 1047–1058. https://doi.org/10.1071/FP08062

Zhang, M. I. N., Willison, J. H. M., & Willison, J. H. M. (1991). Electrical impedance analysis in plant tissues. *Journal of Experimental Botany*, *42*, 1465–1475. https://doi.org/10.1093/jxb/42.11.1465

Zhao, P.-F., Wang, Y.-Q., Yan, S.-X., Fan, L.-F., Wang, Z.-Y., Zhou, Q., … Huang, L. (2019). Electrical imaging of plant root zone: A review. *Computers and Electronics in Agriculture*, 167. https://doi.org/10.1016/j.compag.2019.105058

Zhou, Q. Y., Shimada, J., & Sato, A. (2001). Three-dimensional spatial and temporal monitoring of soil water content using electrical resistivity tomography. *Water Resources Research*, *37*, 273–285. https://doi.org/10.1029/2000WR900284

Zimmermann, E., Kemna, A., Berwix, J., Glaas, W., Münch, H. M., & Huisman, J. A. (2008). A high-accuracy impedance spectrometer for measuring sediments with low polarizability. *Measurement Science and Technology*, *19*(10). https://doi.org/10.1088/0957-0233/19/10/105603

How to cite this article: Ehosioke S , Nguyen F, Rao S, et al. Sensing the electrical properties of roots: A review. *Vadose Zone J.* 2020;19:e20082. https://doi.org/10.1002/vzj2.20082